

e-ISSN: 2651-3722

ARALIK/DEC 2024 CİLT/VOLUME 7 SAYI/ISSUE 2

# Techno-Science

Scientific Journal Of Burdur Mehmet Akif Ersoy University



**Editor**

Prof. Dr. İsmail KIRBAŞ

**SCIENTIFIC  
JOURNAL OF**

BURDUR MEHMET AKİF ERSOY UNIVERSITY

e-ISSN: 2651-3722

## Scientific Journal of Mehmet Akif Ersoy University

Volume 7, Number 2, 2024

e-ISSN: 2651-3722

### Privilege Holder

Burdur Mehmet Akif Ersoy University

Prof. Dr. Hüseyin DALGAR

Rector

### Journal Board

Editor in Chief

Prof. Dr. İsmail KIRBAŞ

Burdur Mehmet Akif Ersoy University, Faculty of Engineering and Architecture, Burdur, Türkiye

### Co-Editors

Prof. Dr. Serkan BALLI, Burdur Mehmet Akif Ersoy University, Bucak  
Faculty of Computer and Informatics, Burdur, Türkiye

Assoc. Prof. Dr. Ali Özhan AKYÜZ, Burdur Mehmet Akif Ersoy  
University, Bucak Emin Gulmez Vocational School of Technical Sciences,  
Burdur, Türkiye

### Section Editors

Prof. Dr. Bahriye BAŞTÜRK AKAY, Erciyes University, Türkiye

Prof. Dr. Şeref SAĞIROĞLU, Gazi University, Türkiye

Prof. Dr. Ali Ziya ALKAR, Hacettepe University, Türkiye

Prof. Dr. İlker Hüseyin ÇELEN, Tekirdağ Namık Kemal University,  
Türkiye

Prof. Dr. Aytağ ONAN, İzmir Katip Çelebi University, Türkiye

Prof. Dr. Aybars UĞUR, Ege University, Türkiye

Prof. Dr. Cüneyt BAYILMIŞ, Sakarya University, Türkiye

Prof. Dr. Osman Ayhan ERDEM, Gazi University, Türkiye

Prof. Dr. Mustafa YAĞCI, Kırşehir Ahi Evran University, Türkiye

Prof. Dr. Turgay İBRİKÇİ, Adana Alparslan Türkeş Science and  
Technology University, Türkiye

Prof. Dr. Kerem KÜÇÜK, Kocaeli University, Türkiye

Prof. Dr. Mehmet YILDIRIM, Kocaeli University, Türkiye

Prof. Dr. Fahri VATANSEVER, Bursa Uludağ University, Türkiye

Prof. Dr. Sezgin KAÇAR, Sakarya University of Applied Sciences,  
Türkiye

Prof. Dr. İlyas ÇİÇEKLI, Hacettepe University, Türkiye

Prof. Dr. Ahmet UYUMAZ, Burdur Mehmet Akif Ersoy University,  
Türkiye

Prof. Dr. Nadir YILMAZ, Howard University, U.S.A.

Prof. Dr. Ahmet ÇİÇEK, Burdur Mehmet Akif Ersoy University, Türkiye

Prof. Dr. Mehmet TOPAKCI, Akdeniz University, Türkiye

Prof. Dr. Arif Behiç TEKİN, Ege University, Türkiye

Prof. Dr. Ecir Uğur KÜÇÜKSİLLE, Süleyman Demirel University,  
Türkiye

Prof. Dr. Uğur BAYSAL, Hacettepe University, Türkiye

Prof. Dr. Murat EFE, Ankara University, Türkiye

Prof. Dr. Devrim AKGÜN, Sakarya University, Türkiye

Prof. Dr. Afşin GÜNGÖR, Akdeniz University, Türkiye

Prof. Dr. Mehmet Fatih AKAY, Çukurova University, Türkiye

Prof. Dr. Ali SEBETCİ, Ostim Technical University, Türkiye

Prof. Dr. Gökhan ŞENGÜN, Atılım University, Türkiye

Assoc. Prof. Dr. Utku KÖSE, Isparta Süleyman Demirel University,  
Türkiye

Assoc. Prof. Dr. Petre LAMESKİ, University of Sts. Cyril and  
Methodius in Skopje, Macedonia

Assoc. Prof. Dr. Yalçın İŞLER, İzmir Katip Çelebi University, Türkiye

Assoc. Prof. Dr. Emrah HANÇER, Burdur Mehmet Akif Ersoy  
University, Türkiye

Asst. Prof. Dr. Ensar Arif SAĞBAŞ, Muğla Sıtkı Koçman University,  
Türkiye

Asst. Prof. Dr. Bora ASLAN, Kırklareli University, Türkiye

Asst. Prof. Dr. Ahmet ÇİFTCİ, Burdur Mehmet Akif Ersoy University,  
Türkiye

Dr. Azim Doğuş TUNCER, Cooling Photonics S. L., Spain

### Language Editors

Assoc. Prof. Dr. Ali Özhan AKYÜZ, Burdur Mehmet Akif Ersoy  
University, Türkiye

Res. Assist. Ali Tezcan SARIZEYBEK, Burdur Mehmet Akif Ersoy  
University, Türkiye

### Secretary

Res. Assist. Ömer Can ESKİCİOĞLU, Burdur Mehmet Akif Ersoy  
University, Bucak Faculty of Computer and Informatics, Burdur, Türkiye

### Redactor

Res. Assist. Mehmet Furkan AKÇA, Burdur Mehmet Akif Ersoy  
University, Bucak Faculty of Computer and Informatics, Burdur, Türkiye

## Contents

### -Research Articles

- Effect of Fuel Injection Parameters on Engine Performance in A Conventional Single Cylinder Spark Ignition Engine** **57**  
Recep Çağrı Orman
- A Healthcare Monitoring System Design for Elderly Living Alone** **81**  
Özlem Coşkun
- Wideband Microstrip Patch Antenna Design At 2.4 Ghz Frequency for Wireless Communication** **91**  
Özlem Coşkun, Nazlıhan Erginyürek
- Development of an Artificial Intelligence Based Correction System for Spelling Errors in Product Reviews** **99**  
Okan Çiğçi, Sumru Nayir, Emre Tolga Ayan, Ceren Ulus, Mehmet Fatih Akay
- Using Musical Notes and Artificial Intelligence Together as a Tool in Spatial Design** **109**  
Hüseyin Samet Aşıkutlu, Latif Gürkan Kaya, Betül Halime Uzunay

### -Review Articles

- The Effects of Agricultural Tire Technologies on Soil Compaction, Traction Performance and Agricultural Productivity** **64**  
Onur Karaçay, Süleyman Kılıç

# Effect of Fuel Injection Parameters on Engine Performance in A Conventional Single Cylinder Spark Ignition Engine

Recep Çağrı ORMAN<sup>1\*</sup> 

<sup>1</sup>Department of Machinery and Metal Technology, Vocational School of Technical Sciences, Gazi University, Ankara, Türkiye

## ABSTRACT

In this study, a 1D model was created using the Ricardo-Wave program for a single-cylinder, spark ignition, four-stroke, direct injection engine with a stroke volume of 398 cc. Air-fuel ratio (AFR), mixture temperature (MT), and start of injection (SOI) were used as fuel injection parameters. Using these parameters, 343 different cases were created. Brake power, thermal efficiency, and fuel consumption were used as engine performance parameters. By holding one injection parameter constant, a contour plot was created to examine the effect of the other two parameters on the engine performance parameter. According to the results, the effect of MT and SOI on brake power is 1%, the effect of AFR on brake power is 9.6%, the effect of MT and SOI on thermal efficiency is 1%, and the effect of AFR on thermal efficiency is 12.8%. The effect of MT and SOI on fuel consumption is 0.04%, the effect of AFR on fuel consumption is 22.9%, and the effect of AFR on brake specific fuel consumption is 22.9%. These results indicate that the most significant effect is provided by AFR, while MT and SOI also have a slight impact on engine performance.

**Keywords:** Fuel injection, Internal combustion engine, Performance, Simulation

## 1. INTRODUCTION

One of the greatest inventions affecting humanity is undoubtedly internal combustion engines. Although many researchers have made significant contributions to the development of internal combustion engines, the historical achievements in the development of the spark-ignition engine (1876) and the compression-ignition engine (1892) have shaped the present of the global automotive industry [1]. These fossil fuel-powered internal combustion engines provide approximately 25% of the world's power. Significant technological advancements have been made in internal combustion engines, particularly in recent years. However, the reputation of internal combustion engines has recently taken a significant hit, primarily due to high-profile emission scandals like the Volkswagen diesel scandal. These scandals revealed that some manufacturers manipulated emissions testing to make their engines appear cleaner than they actually are. This deception has not only damaged trust in these engines but also raised doubts about their potential to contribute meaningfully to future emission reductions, as they have been shown to produce more pollutants under real-world conditions than previously claimed. Consequently, there have been developments aimed at replacing internal combustion engine vehicles with electric drives to further reduce fuel consumption and emissions and decrease vehicle greenhouse gas emissions [2]. For example, in the United Kingdom, internal combustion engine vehicles produced 23% of carbon dioxide emissions in 2010, compared to 14% in 1980 [3]. Although there has been a transition from internal combustion engine vehicles to electric vehicles today, significant work continues internal combustion engines. Society continues to rely heavily on integrated circuit engines for transportation, commerce, and energy production. This is why motor research, with over a century-long history, is still vibrant today. Internal combustion engines are used not only in the transportation sector but also in many areas such as pumps, lawnmowers, chainsaws, and power generators [4]. Changes in motor technology and transportation energy demand, driven by the need to increase the efficiency of internal combustion engines and reduce emissions, also affect future fuel characteristics. The increasing energy demand for transportation is shifting towards jet fuel compared to gasoline [5].

Various simulation programs are used to develop internal combustion engines. Through simulation, the impact of engine design parameters on performance can be observed [6]. 1D engine models are frequently preferred in engine

\*Corresponding Author Email: [recepcegriorman@gmail.com](mailto:recepcegriorman@gmail.com)

Submitted: 23.06.2024 Revision Requested: 13.08.2024 Last Revision Received: 25.08.2024

Accepted: 11.09.2024 Published Online: 11.10.2024



Cite this article as: Orman, R. Ç. (2024). Effect of Fuel Injection Parameters on Engine Performance in A Conventional Single Cylinder Spark Ignition Engine. Scientific Journal of Mehmet Akif Ersoy University, 7(2): 57-63.

DOI: <https://doi.org/10.70030/simakeu.1503849>

<https://dergipark.org.tr/simakeu>



Content of this journal is licensed under a Creative Commons Attribution-NonCommercial 4.0 International License.

analyses. Yontar and Doğu [7], in their study, created a 1D engine model alongside experimental work to observe the impact of CNG and gasoline fuels on engine performance. A 1D model was created for all test equipment and the engine using Ricardo-Wave software, and numerical engine analyses were performed. The same test parameters were analyzed, and the same test outputs were calculated in the 1D engine model. Therefore, the test and 1D engine model were used to measure the effects of gasoline and CNG fuels on engine performance and emissions for a unique engine [7]. Claywell et al., in their study, used Ricardo-Wave software to investigate the performance of the three most common intake concepts for a naturally aspirated four-cylinder Formula SAE engine, as well as the performance of two variations of the basic concepts [8]. Deighan et al., in their study, presented an approach to model engine crankcase gas flow using Ricardo-Wave software. The model was developed and validated using pressure and leakage data during the design of a racing engine's dry sump version. The model was used to measure gas velocities, pressure fluctuations, and power loss resulting from the pumping of crankcase gas [9]. Youssef et al., in their study, created a computer simulation using Ricardo-Wave software to predict the performance and nitrogen oxide emissions of a diesel engine running on a diesel-biodiesel blend and diethyl ether as a fuel additive. The model created was validated with experimental data.

In 1D models, it is common to validate the engine operating conditions with experimental data. However, 1D models can also be created to examine the impact of engine parameters on engine performance. Due to the numerous variables in these models, it may not be possible to validate all obtained data. However, these models can be actively used to observe the impact of a parameter. The main aim of this study was to examine the impact of fuel injection parameters on engine performance in a conventional, single-cylinder, spark-ignition engine using a 1D model.

## 2. MATERIALS AND METHODS

In this study, a 1D model was created in the Ricardo-Wave program for a single-cylinder, spark ignition, four-stroke, direct injection engine with a stroke volume of 398 cc. The engine has two valves. The connecting rod/crank ratio is 3.66. The nozzle diameter of the injector is 0.2 mm and the working pressure is 2000 kPa. In the model, the case in which the engine operates at a constant speed of 5000 rpm is examined. For reference, the air/fuel ratio is 14.5, the fuel-air mixture temperature is 320 K, and the injection start is  $-100^{\circ}\text{CA}$ .

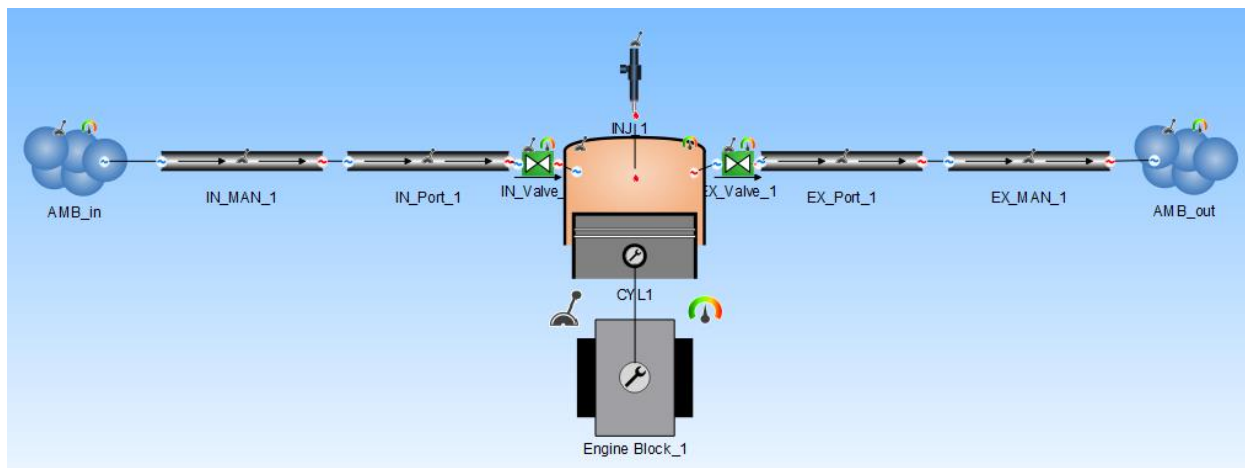


**Fig 1.** Model created for the engine

The change of in-cylinder pressure and temperature to the reference values of the engine is as shown in Fig. 2. The maximum pressure of the engine is 6300 kPa and the maximum temperature is 2650 K. The results of the engine according to these reference values are among the examples tested in the Ricardo-Wave program.

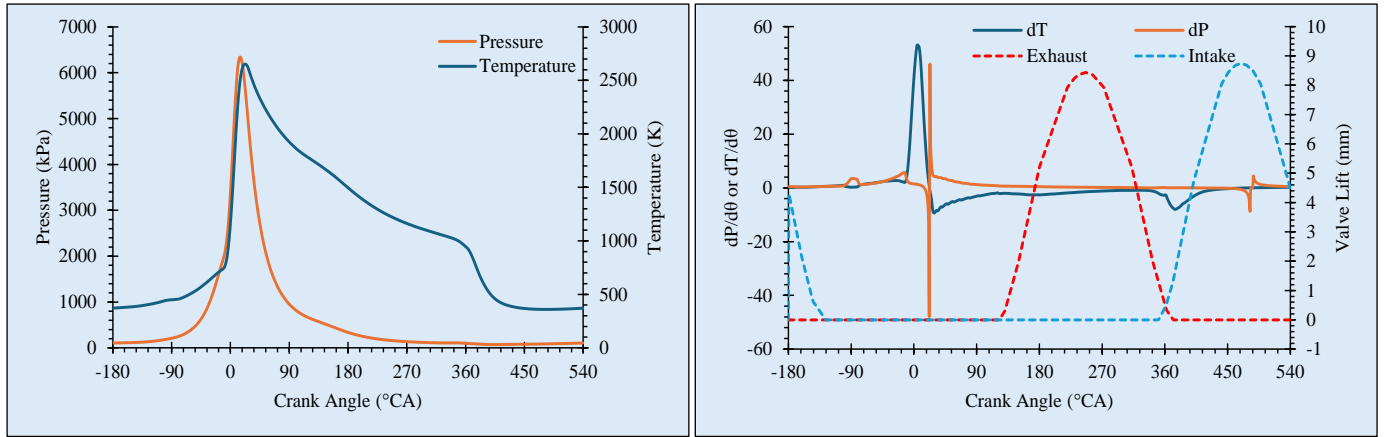


**Fig 2.** In-cylinder pressure and temperature change for reference case

For this study, the injection parameters were air-fuel ratio (AFR) (0.5 step between 13 and 16), mixture temperature (MT) (10 K step between 290 and 350 K), start of injection (SOI) (-130°CA to 10 steps between -70°C) are preferred. 343 full factorial cases were obtained for the parameters in the model. Accordingly, effective power, thermal efficiency and fuel consumption values at 5000 rpm were examined. The term “mixture temperature” here essentially corresponds to “fuel temperature”. The reason for insisting on using 'mixture temperature' instead of 'fuel temperature' is to align with the terminology used in the program. Since the program evaluates parameters for both port injection and direct injection, fuel temperature is referred to as mixture temperature. Actually, fuel temperature is a parameter that directly influences mixture temperature. When fuel is injected into the compressed air, the mixture temperature will decrease slightly due to the evaporation enthalpy of the fuel molecules. If the fuel is hot, some of the energy required for evaporation will be carried into the cylinder with the fuel, which can slightly affect performance. Although fuel temperature is not commonly used as a parameter in practice today, it is known that fuel temperature increases due to pressurization. However, the fuel may cool down in the distance between the pump and the injector. For this reason, mixture temperature has been deliberately considered a parameter in this study, and its impact has been examined.

### 3. MODEL OUTPUTS

The effect of the three determined injection parameters on engine performance was shown by creating contour plots while a certain injection parameter was at the reference value (AFR = 14.5, SOI = -100°CA and MT = 320 K), and the effect of the other two parameters on engine performance was demonstrated.

The effect of injection parameters on braking power is shown in Figure 3. Low AFR and high MT values improve braking power. Figure 3a shows the effect of AFR and MT on braking power when SOI is constant. In this case, it can be seen that MT does not have a significant effect on braking power. However, it is seen that the brake power increases for the case where AFR is low. Figure 3b shows the effect of AFR and SOI on braking power when MT is constant. In this case, it appears that SOI has no significant effect on braking power. However, it is seen that the brake power increases for the case where AFR is low. Here it can be seen that AFR has a dominant effect on braking power. Figure 3c shows the effect of MT and SOI on braking power when AFR is constant. In this case, thermal efficiency increases when MT and SOI are low. A low SOI means the injection starts early. The effect of MT and SOI on braking power is 1%. The effect of AFR on braking power is 9.6%.

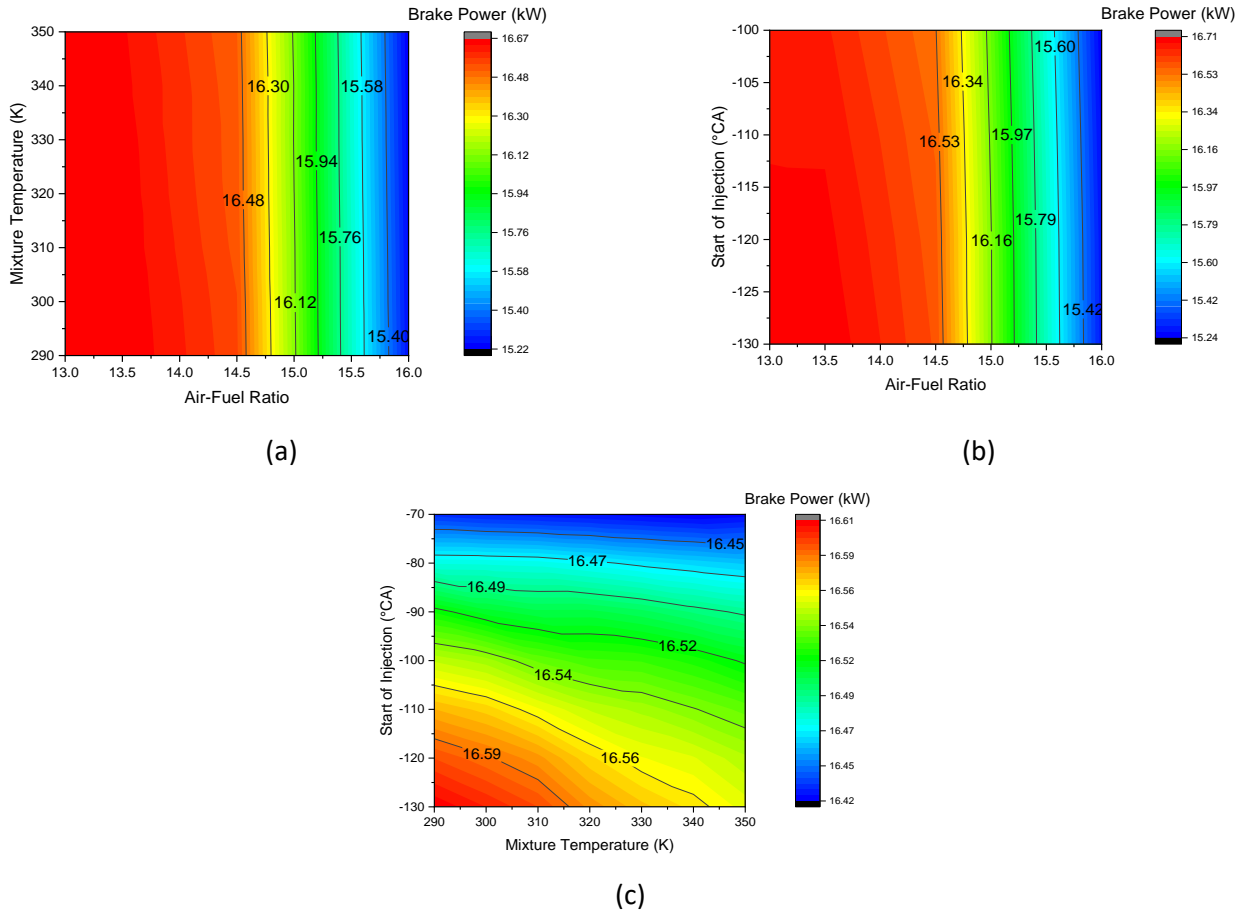


**Fig 3.** Effect of injection parameters on brake power

The effect of injection parameters on thermal efficiency is shown in Figure 4. High AFR and low MT values improve thermal efficiency. Figure 4a shows the effect of AFR and MT on thermal efficiency when SOI is constant. In this case, it appears that MT does not have a significant effect on thermal efficiency. However, it is seen that thermal efficiency increases for the case where AFR is high. Figure 4b shows the effect of AFR and SOI on thermal efficiency when MT is constant. In this case, it appears that SOI does not have a significant effect on thermal efficiency. However, it is seen that thermal efficiency increases for the case where AFR is high. Here it can be seen that AFR has a dominant effect on thermal efficiency. Figure 4c shows the effect of MT and SOI on thermal efficiency when AFR is constant. In this case, when MT and SOI are low, brake power increases. A low SOI means the injection starts early. The effect of MT and SOI on thermal efficiency is 1%. The effect of AFR on thermal efficiency is 12.8%.

The effect of injection parameters on fuel consumption is shown in Fig. 5. Low AFR and high MT values increase fuel consumption. Figure 5a shows the effect of AFR and MT on fuel consumption when SOI is constant. In this case, it can be seen that MT does not have a significant effect on fuel consumption. However, it is seen that fuel consumption decreases when AFR is high. Figure 5b shows the effect of AFR and SOI on fuel consumption when MT is constant. In this case, it appears that SOI does not have a significant effect on fuel consumption. However, it is seen that fuel consumption decreases when AFR is high. Here it can be seen that AFR has a dominant effect on fuel consumption. Figure 5c shows the effect of MT and SOI on fuel consumption when AFR is constant. In this case, when MT and SOI are high, fuel consumption decreases. A high SOI means that the injection starts late. The effect of MT and SOI on fuel consumption is 0.04%. The effect of AFR on fuel consumption is 22.9%.

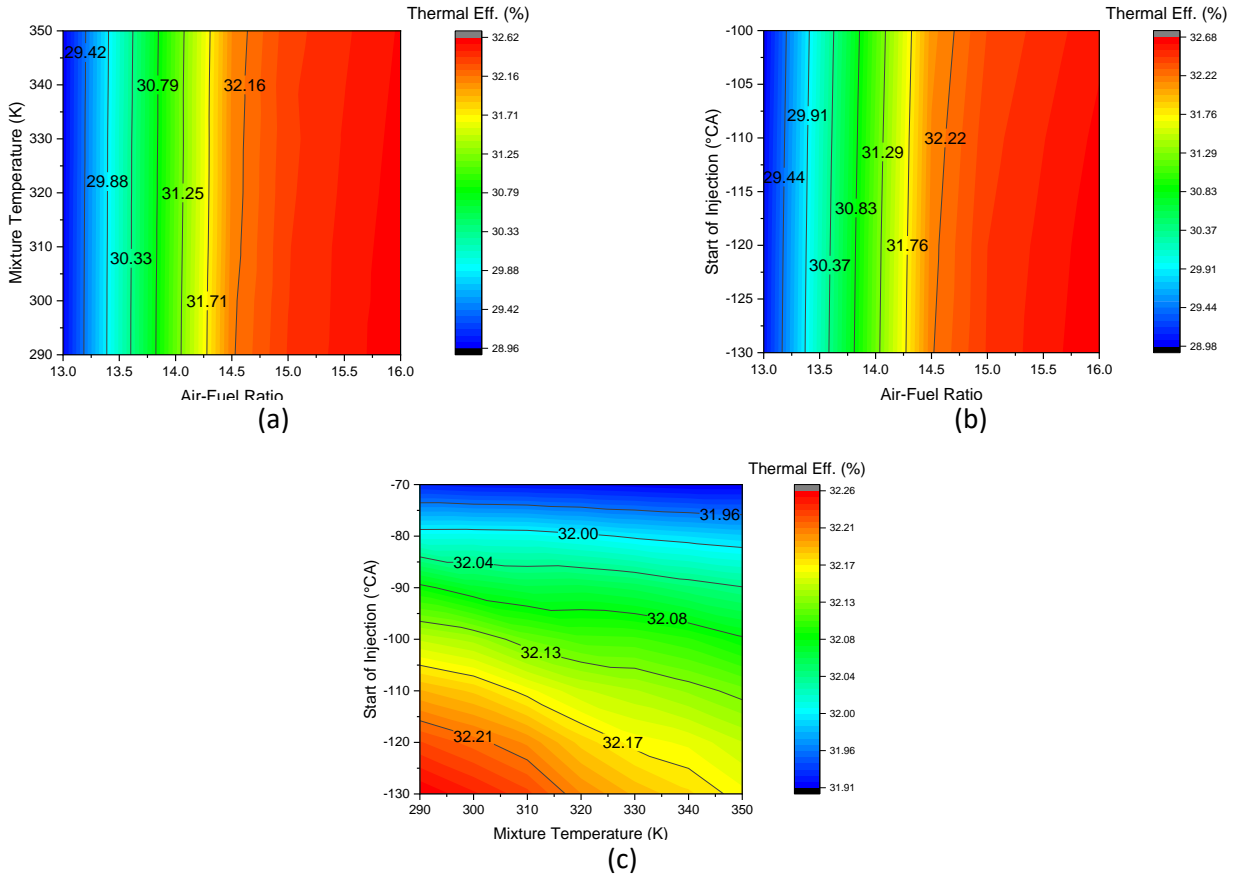


**Fig 4.** Effect of injection parameters on thermal efficiency

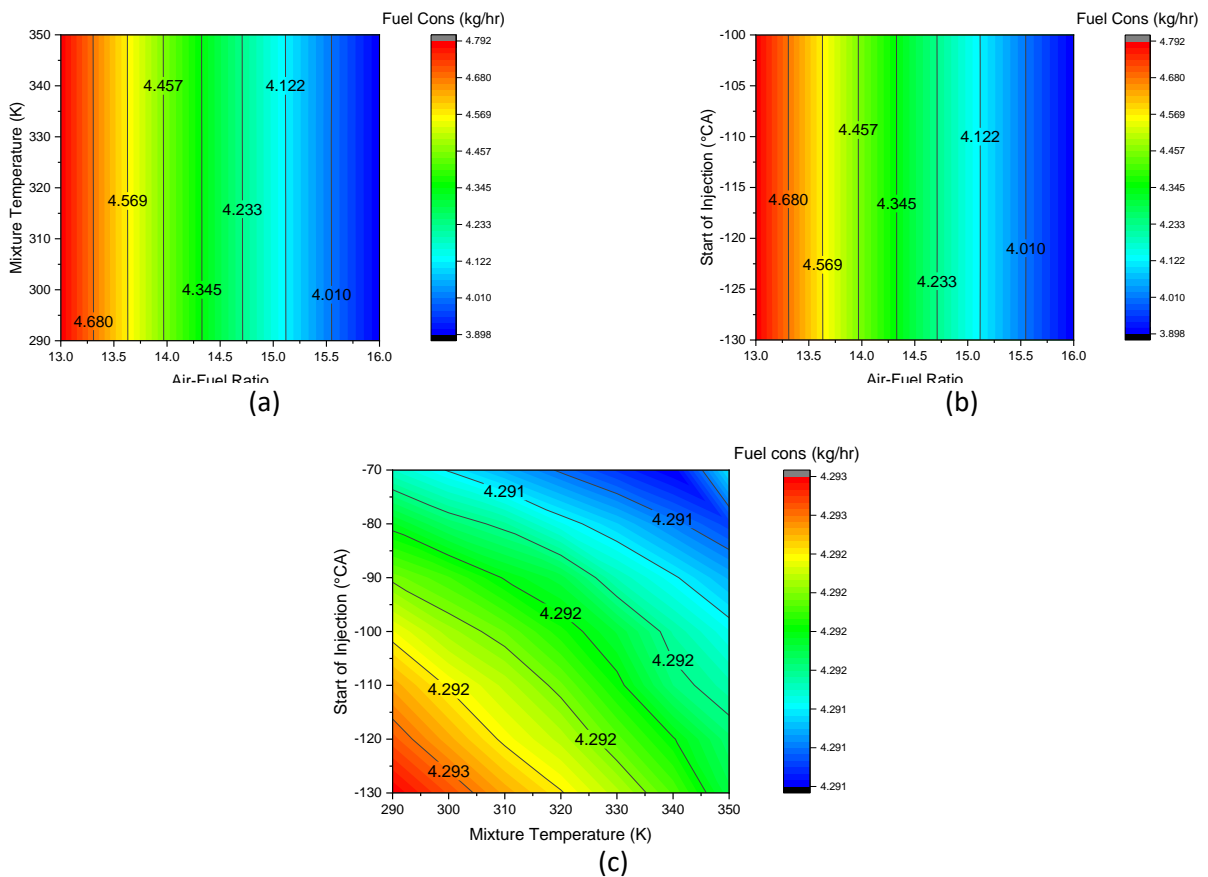


**Fig 5.** Effect of injection parameters on fuel consumption



The effect of injection parameters on brake specific fuel consumption is shown in Fig. 6. High AFR and low SOI values decrease fuel consumption. Figure 6a shows the effect of AFR and MT on brake specific fuel consumption when SOI is constant. In this case, it can be seen that MT does not have a significant effect on brake specific fuel consumption. However, it is seen that specific fuel consumption decreases when AFR is high. Figure 6b shows the effect of AFR and SOI on fuel consumption when MT is constant. In this case, it appears that SOI does not have a significant effect on brake specific fuel consumption. However, it is seen that brake specific fuel consumption decreases when AFR is high. Here it can be seen that AFR has a dominant effect on brake specific fuel consumption. Figure 6c shows the effect of MT and SOI on fuel consumption when AFR is constant. In this case, when MT and SOI are low, fuel consumption decreases. A low SOI means that the injection starts early. The effect of MT and SOI on brake specific fuel consumption is 0.04%. The effect of AFR on brake specific fuel consumption is 12.6%.

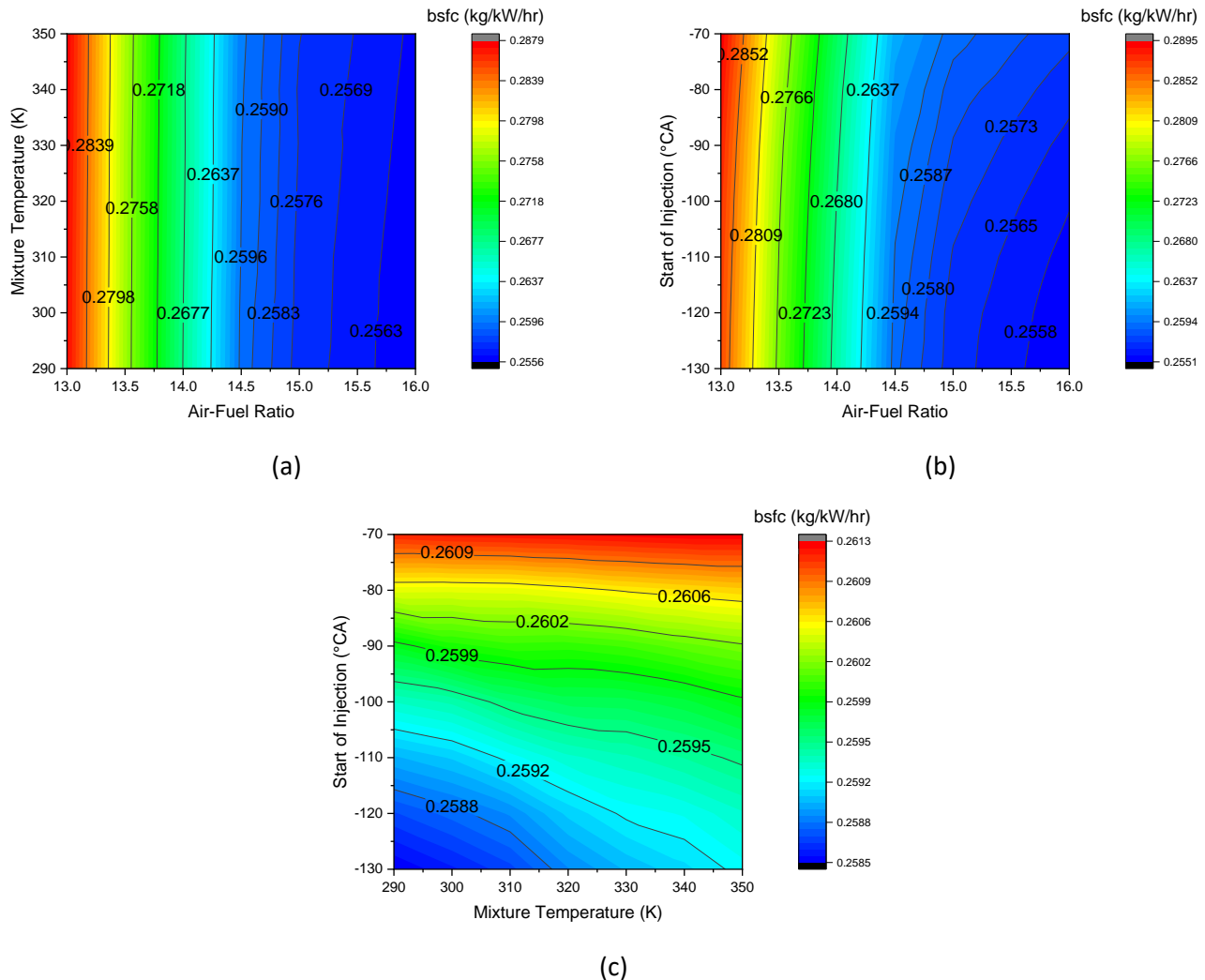



**Fig 6.** Effect of injection parameters on brake specific fuel consumption

#### 4. CONCLUSIONS

In this study, a 1D model was created in the Ricardo-Wave program for a single-cylinder, spark ignition, four-stroke, direct injection engine with a stroke volume of 398 cc. Air-fuel ratio (AFR), mixture temperature (MT) and start of injection (SOI) were used as fuel injection parameters. Using these parameters, 343 different cases were created. Brake power, thermal efficiency and fuel consumption were used as engine performance parameters. By leaving any injection parameter constant, a contour plot was created in which the effect of the other two parameters on the engine performance parameter could be examined. According to the results, the effect of MT and SOI on brake power is 1%, the effect of AFR on brake power is 9.6%, the effect of MT and SOI on thermal efficiency is 1%, the effect of AFR on

thermal efficiency is 12.8%, the effect of MT and SOI on thermal efficiency is 12.8%. The effect of AFR on fuel consumption is 0.04%, the effect of AFR on fuel consumption is 22.9%, and the effect of AFR on brake specific fuel consumption is 12.6%. Here it can be seen that the biggest effect is provided by AFR. However, MT and SOI are also slightly effective on engine performance.

## ORCID

Recep Çağrı ORMAN  <https://orcid.org/0000-0002-7700-2800>

## REFERENCES

- [1]. Alagumalai, A. (2014). Internal combustion engines: Progress and prospects. *Renewable and Sustainable Energy Reviews*, 38, 561-571. <https://doi.org/10.1016/j.rser.2014.06.014>
- [2]. Reitz, R. D., Ogawa, H., Payri, R., Fansler, T., Kokjohn, S., Moriyoshi, Y., ... & Zhao, H. (2020). IJER editorial: The future of the internal combustion engine. *International Journal of Engine Research*, 21(1), 3-10. <https://doi.org/10.1177/1468087419877990>
- [3]. Taylor, A. M. (2008). Science review of internal combustion engines. *Energy policy*, 36(12), 4657-4667. <https://doi.org/10.1016/j.enpol.2008.09.001>
- [4]. Reitz, R. D. (2013). Directions in internal combustion engine research. *Combustion and Flame*, 160(1), 1-8. <https://doi.org/10.1016/j.combustflame.2012.11.002>
- [5]. Kalghatgi, G. T. (2015). Developments in internal combustion engines and implications for combustion science and future transport fuels. *Proceedings of the combustion institute*, 35(1), 101-115. <https://doi.org/10.1016/j.proci.2014.10.002>
- [6]. Cordon, D., Dean, C., Steciak, J., & Beyerlein, S. (2007). One-dimensional engine modeling and validation using Ricardo WAVE. Final Report, University of Idaho.
- [7]. Yontar, A. A., & Doğu, Y. (2018). Experimental and numerical investigation of effects of CNG and gasoline fuels on engine performance and emissions in a dual sequential spark ignition engine. *Energy Sources, Part A: Recovery, Utilization, and Environmental Effects*, 40(18), 2176-2192. <https://doi.org/10.1080/15567036.2018.1495783>
- [8]. Claywell, M., Horkheimer, D., & Stockburger, G. (2006). Investigation of intake concepts for a formula SAE four-cylinder engine using 1D/3D (Ricardo WAVE-VECTIS) coupled modeling techniques (No. 2006-01-3652). SAE Technical Paper. <https://doi.org/10.4271/2006-01-3652>
- [9]. Deighan, T., & Zuhdi, N. (2007). Crankcase flow modeling for a racing motorcycle engine (No. 2007-01-0266). SAE Technical Paper. <https://doi.org/10.4271/2007-01-0266>
- [10]. Youssef, A., & Ibrahim, A. (2024). A numerical investigation on enhancing the performance of a diesel engine fuelled with diesel-biodiesel blend using a diethyl ether as an additive. *Engineering Reports*, e12915. <https://doi.org/10.1002/eng2.12915>

*Techno-Science Paper ID: 1503849*

# The Effects of Agricultural Tire Technologies on Soil Compaction, Traction Performance and Agricultural Productivity

Onur KARAÇAY<sup>1\*</sup> , Süleyman KILIÇ<sup>2</sup> 

<sup>1</sup>Institute of Natural and Applied Sciences, Kırşehir Ahi Evran University, Turkey.

<sup>2</sup>Department of Mechanical Engineering, Kırşehir Ahi Evran University, Turkey.

## ABSTRACT

This review article examines the impact of agricultural tire technologies on soil compaction, traction performance, and agricultural productivity. Topics such as the stress distribution of low-inflation pressure tires on soil, the effects of tire profiles on performance and soil compaction are discussed in depth. Moreover, the impact of tires on traction and soil compaction under different inflation pressures is explored. A thorough analysis of the existing literature reveals significant contributions to improving the efficiency of agricultural tires and reducing the risk of soil compaction. The findings reveal that low-inflation pressure next-generation tires (IF/VF tires) significantly reduce soil compaction by providing a larger contact area. Furthermore, it was concluded that selecting the appropriate inflation pressure and load distribution is critical for optimizing traction and energy efficiency. This review provides valuable insights for future studies and contributes to sustainable agricultural practices.

**Keywords:** Agricultural tire technology, Soil compaction, Traction, Agricultural productivity

## 1. INTRODUCTION

Soil compaction is one of the main problems that reduces productivity and negatively affects soil health in modern agricultural practices [1, 2]. Intensive use of agricultural machinery, especially tractors and other heavy equipment, causes the soil pore structure to deteriorate and water-air permeability to decrease due to the stresses they create on the soil. This situation restricts plant root development and negatively affects agricultural production potential [22]. In recent years, agricultural tire technologies developed to minimize these negative effects have provided significant improvements in reducing soil compaction with tires having lower inflation pressure and larger contact surfaces [3].

In the current management system, engine powers reaching 500 KW in tractors are constantly increasing and demands for fuel consumption and greenhouse emissions are increasing. For this reason, tire manufacturers carry out intensive R&D studies on tire designs. The design of agricultural tires not only reduces soil compaction, but also plays an important role in traction, energy efficiency and sustainability of agricultural activities [4]. The distribution of stress applied to soil by tires at various inflation pressures and its effects at different soil depths have been extensively studied in the literature [5]. Research shows that low-inflation-pressure tires distribute soil surface stress over a wider area, reducing compaction and increasing agricultural yields [6]. These types of tires provide a large contact area, allowing the stress applied to the soil surface to be distributed more homogeneously, thus reducing compaction in the lower soil layers. New generation tires with low inflation pressure (for example, Advanced Elasticity (IF) and Very High Elasticity (VF) technology) can operate with lower pressure compared to traditional tires and cause less damage to the soil structure under the same load [7, 8].

\*Corresponding Author Email: [karacay.onur@ogr.ahievran.edu.tr](mailto:karacay.onur@ogr.ahievran.edu.tr)

Submitted: 08.10.2024 Revision Requested: 21.10.2024 Last Revision Received: 24.10.2024

Accepted: 02.11.2024 Published Online: 26.11.2024



Burdur  
Mehmet Akif Ersoy  
University Press



Cite this article as: Karaçay, O., Kılıç, S. (2024). The Effects of Agricultural Tire Technologies on Soil Compaction, Traction Performance and Agricultural Productivity. Scientific Journal of Mehmet Akif Ersoy University, 7(2): 64-80.

DOI: <https://doi.org/10.70030/simakeu.1563596>

<https://dergipark.org.tr/simakeu>



Content of this journal is licensed under a Creative Commons Attribution-NonCommercial 4.0 International License.

By analyzing the relationship between the performance characteristics of agricultural tires and their capacity to prevent soil compaction, important results were obtained for the sustainability of agricultural activities [9]. In this review, the effects of agricultural tire technologies on soil compaction, traction performance and agricultural productivity were examined and the potential contributions of these technologies in future agricultural applications were discussed in the light of existing literature. In particular, further investigation of subsoil layers, calculation of long-term soil compaction effects, and more comprehensive modeling of the effects of tires on energy efficiency could contribute to future studies. The study aims to summarize the current status of the literature on the development of new generation tire technologies in order to guide applications that aim to increase efficiency in agricultural production and minimize soil compaction.

## 2. EFFECT OF PRESSURE, LOAD, GROUND CONDITIONS ON SOIL STRESS IN AGRICULTURAL TIRES

### 2.1 Effect of Low Inflation Pressure Tires on Soil Stress

Damme and colleagues [3] studied the effects of tires with low inflation pressure on soil stress. Soil stress is measured by dividing the force applied to a specific area of soil by the area itself and is expressed as force per unit area (Pa or kPa). The study examined the effect of three different tire types (AxioBib, CerexBib and EvoBib) with similar dimensions, wide and low inflation pressure, on the average stress in the soil profile (Figure 1). They tested the tires under different inflation pressures and wheel loads. The average normal stress was measured at six different locations using probes.



**Fig 1.** Different types of Michelin brand agricultural tires, a-) AxioBib, b-) CerexBib, c-) EvoBib [10]

The results showed that the tire structure had no significant effect on the stress applied to the soil, but reducing the inflation pressure reduced the stress in the upper soil layers. It was found that the effect of inflation pressure was limited in the lower soil layers. It has been noted that there is no significant difference in the center of the front and rear tires. At normal stress values of the rear wheels only at a depth of 0.2 m, the AxioBib tire produced 16-20% lower stress than other tires. This difference was said to be due to testing the CerexBib with low inflation pressure. Lowering the inflation pressure of the EvoBib tire has been shown to decrease mean normal stress, particularly in the upper soil layers. It was emphasized that when it was reduced from 80 kPa to 60 kPa, the stress caused by the front and rear tires decreased by 22%, and when it was reduced from 60 kPa to 40 kPa, the stress caused by the rear tires decreased by 11%. They observed that when the EvoBib tire load was reduced by 20% and the inflation pressure was reduced by 25%, the average normal stress was reduced by 10-14%. However, this decrease was not found to be statistically significant.

The average normal stress on the soil is calculated using Equation 1. In this calculation, the maximum internal pressure  $P_{i-max}$  and the proportionality coefficient  $k_s$ , which is a function of the Poisson ratio, are used. Maximum internal pressure refers to the highest pressure measured in the ground under the load applied by the tire to the ground.

$$\sigma_m = P_{i-max} k_s \approx \frac{P_{i-max}(1-3\nu)}{(1+\nu)} \quad (1)$$

Here  $\nu$  is the Poisson ratio and is obtained from the mechanical properties of the soil. Poisson's ratio ( $\nu$ ) expresses the ratio of the transverse expansion of the material to the longitudinal compression.

The study shows that tires with low inflation pressure significantly reduce soil compaction in the upper soil layers. It was concluded that the tire load was more decisive in the lower soil layers. These findings highlight that inflation pressure is a critical factor. The EvoBib tire in particular has been identified as the most effective tire in reducing stress in the upper soil layers at low inflation pressure. One of the strengths of the study is that it quantitatively models the effect of different inflation pressures. However, the models focus on only the upper soil layers resulted in a less comprehensive examination of the effects on the lower layers. It is thought that future studies should include more in-depth analysis of the subsoil layers.

## 2.2 Tire Slippage Under the Influence of Inflation Pressure in Agricultural Tires

How to optimize the slip and traction efficiency of tractor tires on the ground is an important issue. Janulevičius and Damanauskas (2022) developed an equation to predict tractor tire slippage under different inflation pressures. Traction efficiency reflects the proportion of engine power transferred to the ground as tractive force. High traction efficiency allows the tractor to operate more efficiently with less energy. Tire slippage indicates how much of the force applied to the ground is not being used effectively. High slip rates reduce productivity and cause soil compaction. While low pressure provides a wider contact area, reducing slippage, very low pressure can damage the tire structure. Traction efficiency  $\eta_t$  in tractors can be calculated with Equation 2 depending on the traction coefficient  $\kappa$ , rolling resistance coefficient  $\rho$ , and slip coefficients [11].

$$\eta_t = \frac{\kappa}{\kappa - \rho} (1 - s) \tag{2}$$

The traction coefficient equation ( $\kappa$ ) is calculated with the traction force ( $F_t$ ) and tractor weight ( $W$ ) using Equation 3 [11, 12].

$$\kappa = \frac{F_t}{W} \tag{3}$$

The rolling resistance coefficient ( $\rho$ ) is calculated with the rolling resistance force ( $F_f$ ) and tractor weight ( $W$ ) using Equation 4 [11, 12].

$$\rho = \frac{F_f}{W} \tag{4}$$

The tire slip coefficient ( $s$ ) equation is calculated with the help of the maximum slip value ( $s_{lim}$ ), the critical traction coefficient ( $F_t^{lim}$ ) and a coefficient ( $b$ ) depending on the soil and tire properties, using Equation 5 [4].

$$s = s_{lim} \left[ 1 - \left( 1 - \frac{F_t}{F_t^{lim}} \right)^b \right] \tag{5}$$

The empirical equation they proposed predicted the average slip rate with a 5% error margin. The findings of the study reveal that different inflation pressures have a significant effect on tractor tire slippage. Low inflation pressure allows the tire to contact the ground on a larger surface, reducing slippage and increasing traction efficiency. However, very low pressures can damage the structural integrity of the tire and cause deformation. Future studies should aim to improve these models with larger data sets and under different soil conditions.

Fig 2, generated by the above equations, shows the effect of traction force on traction efficiency and tire slippage. As traction force increases, efficiency increases, but if slippage also increases, efficiency decreases. In Fig 3, it is seen that increasing traction force increases slippage and decreases efficiency.

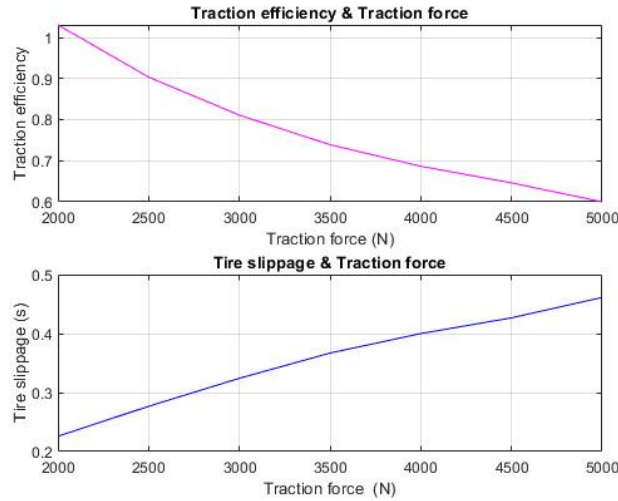


**Fig 2.** Effect of traction force on traction efficiency and tire slip [4]

### 2.3 Effect of Ballast on Different Types of Agricultural Tires

Kumar et al.[13] studied the performance of bias-ply and radial tires in different ballast conditions. Bias-Ply and Radial tire shapes are shown in Fig 3. Ballast is water or iron weights used to increase the weight of the tractor and reduce slipping. In the study, tires of sizes 13.6–28 were tested under different ballast and inflation pressures (68.9–206.8 kPa).



**Fig 3.** Different types of tires, a-) Bias-Ply, b-) Radial [14]

In their study, they tested 13.6–28 Bias-Ply and Radial tires (empty, 50% water, 50% iron, 75% water, 75% iron) and inflation pressures (68.9 - 206.8 kPa) (Fig 4). In their tests, they evaluated the vertical deflection and contact area. Vertical deflection indicates how much the tire flexes in the vertical direction. It varies with the load acting on the tire and inflation pressure. Contact Area refers to the surface area of the tire that comes into contact with the ground. This area changes with the inflation pressure of the tire and the load applied to it.



**Fig 4.** Test tires used in the study, a-) Bias, b-) Radial

Radial tires demonstrated a 13% larger contact area and a 6.5% greater deflection compared to Bias-Ply tires. The results showed that using low inflation pressure and high ballast creates a large contact area for the tire and increases

efficiency. Water ballast provided lower deflection and contact area than iron ballast, while iron ballast performed better under load. Optimization of ballast type and inflation pressure is critical to maximizing tractor efficiency. In the evaluations made using the Commando model, tire performance was analyzed with tire deflection and contact area equations (Equations 6 and 7). The Komandi model [15, 16] is a model used in the analysis of ground-vehicle interactions and evaluates performance by taking into account variables such as normal load ( $W$ ), tire section width ( $b$ ), tire diameter ( $d$ ), and inflation pressure ( $P_i$ ). This model performs performance analysis based on the surface area ( $A$ ) where the tire is in contact with the ground and the amount of vertical deformation of the tire (deflection,  $\delta$ ). It has been found that radial tires provide better load distribution under high weight and low pressure conditions and can be preferred in agricultural applications. It has been observed that radial tires create a more balanced contact area, especially as the load applied to the tire and the tire section width increase. The expanding contact area under low inflation pressure can optimize traction by increasing the amount of deformation (deflection) while reducing soil compaction.

$$\text{Tire deflection } (\delta) (\%) = \left( \frac{\text{Vertical tire deflection}}{\text{Carcass section height}} \right) \times 100 \quad (6)$$

$$\text{Tire deflection } \delta = C1 \times \frac{W^{C2}}{b^{C3} d^{C4} P_i^{C5}} \times (C3 \times b + C4)$$

$$\text{Contact area } A = C1 \times W^{C2} \times \left( \frac{b}{d} \right)^{C3} + P_i^{C4} \quad (7)$$

The findings of the study show that the use of ballast has a significant impact on the performance of both bias and radial tires. However, it is emphasised that the long-term effects of iron and water ballasts need further investigation. The study provides significant contributions to the optimization of tire performance by providing a wide data set obtained with different ballast types and tire types.

## 2.4. Reducing the Risks that may Arise from Soil Compaction with the Developments in the Tire Industry

Soil compaction disrupts the physical structure of the soil and reduces its water and air permeability, as noted by Damme et al.[17]. Investigated how new generation tires can minimize this situation on five generations of tires (1970-2018). In the study, tire loads of 2900 kg and 4300 kg were applied to the tires and the inflation pressure was varied between 240 and 60 kPa. The tire-soil contact area and stress distribution were calculated with the FRIDA model, and the results were compared with the vertical stresses in the soil profile using the Söhne model. The FRIDA model gives the shape and stress distribution of the tire-soil contact area. The Poisson ratio was obtained from the Uniaxial confined compression test (UCCT) slope and Young's modulus.

In their study, the Poisson ratio was determined by a method based on the work of Eggers and colleagues [18]. In this method, the slope of the reloading section (UCCT) and Young's modulus are combined. The load was converted to stress and log10-transformed. Displacement was converted into unit deformation (Equation 8).

$$v = \frac{1}{4} \left[ \frac{d\varepsilon_z}{d\sigma_z} E + \left\{ \left( 1 - \frac{d\varepsilon_z}{d\sigma_z} E \right) \left( 9 - \frac{d\varepsilon_z}{d\sigma_z} E \right) \right\}^{0.5} - 1 \right] \quad (8)$$

The results show that the new generation of tires with low pressure and large contact area significantly reduces soil stress. In particular, the EvoBib tire provided the best stress distribution and low soil compaction. FRIDA model calculations revealed that soil compaction was reduced even at a depth of 0.6 m.

These findings demonstrate the potential for innovations in tire design to both reduce soil compaction and contribute to agricultural sustainability. Tires with large contact surface support plant root development. However, the long-term effects of these technologies in different soil types and load conditions need to be investigated further. Future studies can increase the effectiveness of these technologies with larger data sets under different climate and soil conditions.

## 2.5. Research on Soil Compaction for Effective and Efficient Production in Agricultural Fields

The force applied to the soil by heavy machinery used in agricultural areas disrupts the soil structure and negatively affects productivity and environmental quality. To prevent this situation, Shaheb and et al. [9] examined the methods recommended for sustainable agriculture. While agricultural machinery increases productivity, it can cause soil compaction, which can lead to yield losses of up to 50%. To reduce this negative impact, strategies such as the use of low inflation pressure tires, controlled traffic agriculture and planting of deep-rooted plants are recommended. Low inflation pressure tires minimize soil compaction with a larger contact area.

In parallel with the rapid increase in the world population, food production must also be increased rapidly. New generation agricultural machinery developed for this purpose has become quite widespread. While new generation agricultural machinery facilitates agricultural production, it also damages the soil and causes soil compaction. Soil compaction disrupts the structure of the soil, negatively affecting plant root development, overall plant growth and yield. To prevent soil compaction, which can cause yield losses of up to 50%, the use of low inflation pressure tires, controlled traffic farming and the planting of deep-rooted plants are recommended [9]. Standard and high inflation pressure tires cause more soil compaction than low inflation pressure tires. The use of low inflation pressure tires reduces compaction by creating a larger contact area on the soil.

The negative effects of agricultural machinery on the soil constitute a significant obstacle to sustainable production. Soil compaction prevents the development of plant roots, makes it difficult for water and nutrients to reach the plants, and as a result, leads to productivity losses. Studies by Shaheb et al. [9] have shown that methods such as controlled traffic farming, use of low inflation pressure tires and planting of deep-rooted plants significantly reduce the risk of soil compaction. These strategies are particularly critical to the viability of sustainable agriculture.

The management strategies discussed in this study provide valuable approaches to support sustainable production and minimize the long-term of soil compaction. However, more research is needed on how these methods perform in different soil types and climate conditions. Moreover, the economic viability of these strategies and the rate at which farmers adopt these methods should also be the subject of future studies.

## 2.6. Soil Compaction in Tires Used in Different Conditions

Rodriguez and et al. [6] studied the effects of different types of tires used during sugarcane harvesting and transportation on soil compaction. Factors that determine soil compaction include tire contact area, inflation pressure, tire hardness, load and soil conditions. Four different tire types (block pattern, rib pattern, low tread profile and high tread profile) were tested at three different inflation pressures (207, 276, 345 kPa) and six load levels (20-60 kN) (Fig 5). The contact surface of the tires was measured by leaving marks on the cardboard, and their vertical deflections were recorded with a hydraulic system. Vertical tensions in the soil were monitored with sensors placed at depths of 10, 30, 50 and 70 cm. These stresses were simulated using the Boussinesq equation.

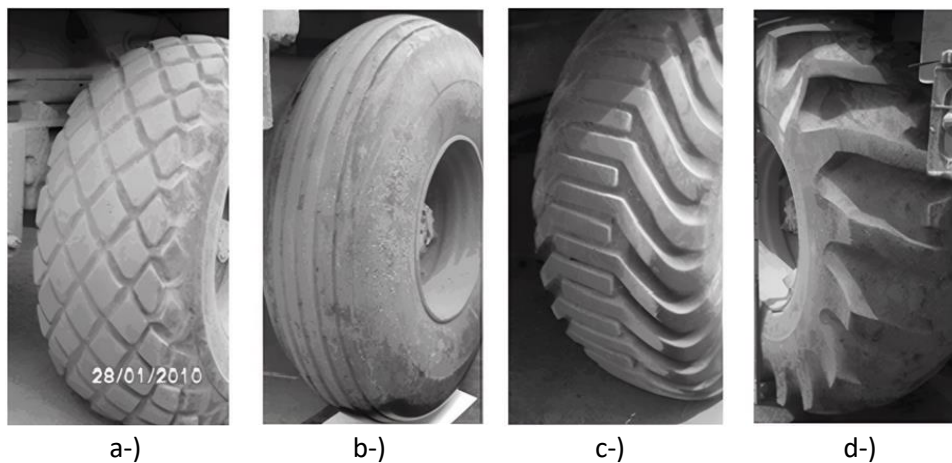


**Fig 5.** Effect of different types of tires on soil compaction. a-) block patterned lug profile, b-) rib patterned lug profile, c-) low lug profile, d-) high lug profile tire



The Boussinesq point load equation is the stresses created by a vertical point load of magnitude P on a surface point at any point at a horizontal distance r in a semi-infinite elastic half-space at a depth of z. Equality 9 expresses the stresses at any point at a horizontal distance r in a semi-infinite elastic half-space [19, 20].

$$\text{Vertical tension } (\sigma_z): \sigma_z = \frac{3P}{2\pi z^2} \left( \frac{z^3}{(r^2+z^2)^{5/2}} \right)$$

$$\text{Horizontal tension } (\sigma_r) = \sigma_r = \frac{P}{2\pi} \left( \frac{3z^3 r}{(r^2+z^2)^{5/2}} \right) \quad (9)$$

$$\text{Shear stress } (\tau_{zr}) = \tau_{zr} = \frac{3P}{2\pi} \left( \frac{z^2 r}{(r^2+z^2)^{5/2}} \right)$$

The contact surface area ( $A_t$ ) was calculated based on the tire width ( $B_s$ ) and diameter ( $D_e$ ) with the McKyes model (McKyes 1985). Type A (block pattern) and type B (rib pattern) tires create lower contact pressure and vertical tension, causing less damage to the soil. As the load increases, the contact surface expands, and as the pressure increases, the contact area shrinks. While the B type tire stands out as the most sensitive tire to different pressure and load changes, the D type tire produced high contact pressure on hard surfaces. A and B type tires minimize soil compaction during transportation.

$$A_t = \frac{B_s \times D_e}{k} \quad (10)$$

$k$  = Although there is a fixed value for the surface type, it is used as 4 for hard surfaces and 2 for loose soils.

The measurement results of soil compaction agreed with the simulation data by 87-92%, demonstrating the reliability of the mathematical models. It was determined that A and B type tires offered better performance in sugar cane transportation with lower contact pressure and more balanced stress distribution.

As a result, A and B type tires are among the best choices for agricultural applications, with less damage to the soil under low inflation pressure and high load conditions. However, further investigation of the performance of these tires in different soil conditions and their long-term effects are required. Future studies should examine the effectiveness of these tires in different agricultural practices and evaluate their contributions to sustainable agriculture.

## 2.7. Effect of Change in Tire Inflation Pressure on Rating Cone Curve (RCI) Index

It is important to correctly assess the impacts of agricultural machinery on the soil and the soil's response to these impacts. Oh et al. [21] studied the effects of tire inflation pressure on the rating cone index (RCI). RCI is an indicator that determines the impact of machinery on the soil and the strength capacity of the soil. In their study, tire inflation pressure was changed between 50-150% and real-time tire penetration depth was measured using laser distance sensors. Wheel rotations were monitored using a rotary encoder, and tire slippage was calculated by comparing theoretical and actual travel distances.

The RCI value was calculated depending on the tire load (W), tire slip ratio (s), tire indentation depth (z), tire width (b), diameter (d) and tire deflection amount ( $\delta$ ) (Equation 11). As inflation pressure increased, tire penetration depth and slip rate increased, but beyond the optimum pressure level these changes slowed down. The study showed that the RCI value increased with increasing tire inflation pressure, but these changes stabilized outside the optimum pressure range (90-120%). The average estimation error rate in RCI calculations was found to be 1.59%.

$$RCI = 2,6265 \left( \frac{W(1 - \frac{\delta}{h})^{3/2}}{bd^{2/5}} \right) \left( \frac{s}{z^3} \right)^{1/3} \quad (11)$$

The distance of the rear sensor to the tire tread profile ( $h_r$ ), the average vertical distance of the front sensor to the tread profile ( $h_f$ ) and the vertical distance between the ö and rear sensors ( $\Delta$ ) are calculated with Equation 12 for the tire penetration depth ( $z$ ).

$$z = \frac{h_r - (h_f \pm \Delta)}{2} \quad (12)$$

Tire slip ( $s$ ) is calculated with the help of Equation 13 using the equation of the actual movement distance of the tractor ( $S_a$ ) and the theoretical movement distance of the tractor ( $S_t$ ).

$$s = 1 - \frac{S_a}{S_t} \quad (13)$$

These equations and calculations are used to better understand soil and machinery interactions and to minimize the negative effects of agricultural machinery on the soil. Accurate RCI estimates are important to prevent soil compaction and increase agricultural productivity.

The results showed that as inflation pressure increases, the risk of soil compaction increases, but more consistent and lower deflection values are obtained within the optimum pressure range. Low inflation pressure below the optimum pressure level increased tire deflection and sinking. The change of RCI values at different pressure levels revealed that inflation pressure is an important parameter in minimizing the negative impact of agricultural machinery on the soil.

This study highlights the impact of tire inflation pressure on RCI and how strategies should be developed to reduce the negative impacts of agricultural machinery on soil. However, these findings need to be extended under different soil types and field conditions. It is also recommended to investigate the potential to increase energy efficiency in agricultural production by optimizing inflation pressure.

## 2.8. Estimation of Carcass Stiffness in Agricultural Tires

The increase in the power and weight of agricultural machinery increases soil compaction and reduces productivity. Misiewicz et al. [22] compared four different methods to estimate the carcass stiffness of agricultural tires. The methods examined are: footprint area, tire load and deflection, pressure mapping, and manufacturer specifications.

- i. Contact Area Method: The contact area of the tire is determined using ink and the average contact pressure is calculated. The contact pressure values obtained with this method were found to be 30-40% lower than the pressure mapping method.
- ii. Tire Load and Deflection Method: As the load increases, the deflection increases and the slopes show a linear relationship with the pressure.
- iii. Pressure Mapping Method: Average and maximum contact pressure is measured using a commercial system. It has been found to be the most accurate and effective in measuring carcass hardness.
- iv. Manufacturer Specification Method: Carcass hardness is estimated from data provided by the manufacturer. This method provided simple and rapid results and showed agreement with other methods within  $\pm 20\%$ .

The results showed that the pressure mapping system provided the most accurate estimates, while the method based on manufacturer data provided a simple and fast alternative. However, the methods need to be tested with large data sets and different tire types. Additionally, it is important to evaluate the accuracy of the methods in real-world conditions in the field.

## 2.9. Effects of Tire Systems Used in Different Agricultural Vehicle Types on Soil Compaction and Traction Power

Arvidsson et al. [23] studied the effects of rubber track systems used in agricultural tractors on soil compaction and traction performance. An example rubber track system is given in Figure 6. The study was carried out in Sweden in 2009 on two different clay soils with an 85 kW tractor. Tractor equipped with four track units, compared with single and twin wheel configurations. In measurements made at depths of 15, 30 and 50 cm, it was found that tracks and double wheels created similar soil stress, while single wheels caused higher soil stress.



**Fig 6.** Tractor track tire system [24]

Track systems provide a larger contact area, reducing soil stress and significantly reducing slippage. Dual wheels reduced slip rates in compact soils, but this effect was limited in loose soils. Single wheels created higher stress levels at all depths, increasing the risk of soil compaction. The stress difference created by the pallets and double wheels at a depth of 50 cm was minimal.

The study results show that rubber track systems increase the efficiency of tractors while causing less damage to the soil and minimizing compaction. With their large contact surface, the pallets distributed the pressure applied to the soil and reduced the risk of soil compaction, which provided a significant advantage in terms of agricultural sustainability.

However, further investigation of the performance of these systems under different soil types and operating conditions is required. Assessing the long-term cost and sustainability impacts of pallet systems could enable greater adoption of these technologies in agriculture.

### 2.10. Modelling of Compressive Strength Between Rubber and Soil in Different Soil Types

Soil compaction occurs as a result of the pressure exerted on the soil by heavy machinery and negatively affects plant root development, making it difficult to absorb water and nutrients. High flexibility (IF) and very high flexibility (VF) tires have been developed to reduce soil compaction with low ground pressure and support heavy loads. Jjagwe et al. [25] studied the pressure-sinkage relationship using plates of different geometric shapes (circular, rectangular and square) on artificial soil. Pressure-sinking data were analyzed with Bekker and Reece models in experiments conducted in loose and dense soil conditions.

While the Bekker model estimates the pressure-sinking relationship by taking into account the cohesion ( $k_c$ ) and friction moduli ( $k_\phi$ ) of the soil, the Reece model examines the compatibility of these parameters to geometric scaling. In loose soil, the pressure increase follows a more linear course, while in dense soil an exponential increase is observed. Both models were able to predict pressure and subduction depths successfully, with the Reece model giving better results in plate-soil interaction.

Bekker Model

$$p = \left( \frac{k_c}{b} + k_\phi \right) z^n = k_{eq} z^n \quad (14)$$

Reece Model

$$p = (Ck'_c + \gamma_s b k'_\phi) (z/b)^{n'}$$

The parameters used in the equations are as follows:  $p$  represents the pressure (kPa),  $b$  represents the small size of the plate (in meters) and  $z$  represents the subduction depth (in meters). While  $k_c$ , which defines the mechanical properties of the soil, is the cohesion modulus of the soil and is shown in the unit  $[kN/m^{n-1}]$ ,  $k_\phi$  defines the friction modulus as  $[kN/m^n]$ .  $k_{eq}$  represents the equivalent parameter between the soil and the plate. The apparent cohesion of the soil is expressed as  $C$  (in kPa) and the soil weight density is defined as  $\gamma_s$   $[kN/m^3]$ . The parameters of the Reece model,  $k_c'$  and  $k_\phi'$ , denote the dimensionless soil cohesion and friction modul, respectively. Finally,  $n'$  is the parameter representing the soil exponent in the Reece pressure-sinking relationship.

The results showed that plate geometry and soil density have significant effects on the pressure-sinking relationship. Circular and rectangular plates produced lower compressive strength than square plates. These studies provide useful data for minimizing soil compaction in the design of agricultural machinery. However, the validity of these models needs to be tested in real agricultural areas. Future studies should improve the accuracy of model predictions with larger data sets and evaluate their long-term effects.

### 2.11. Modelling of Footprint and Vertical Stress Distribution in Agricultural Tires

When vehicles move over the ground, the ground surface is exposed to mechanical stresses from the tires. This stress varies depending on tire inflation pressure, wheel load, tire dimensions and soil conditions. To accurately predict the impact of agricultural machinery on soil, modeling of the tire-soil contact area and vertical stress distribution is necessary. Keller [5] developed an approach that models the contact area and stress distribution based on tire parameters. The model describes the contact area with a super ellipse, the longitudinal distribution of vertical stress with a power law function, and the transverse distribution with a decay function.

In this model, pressure sensors placed on the soil surface were used to calculate vertical stress and the obtained data were analyzed with Boussinesq and Fröhlich equations [19, 26]. The maximum vertical stress is related to the tire inflation pressure ( $P_{tyre}$ ), wheel load ( $F_{wheel}$ ) and the logarithm of the recommended tire pressure ( $P_{recommended}$ ) and is described by the equation:

$$\sigma_{max} = 34.4 + 1.13P_{tyre} + 0.72F_{wheel} - 33.4 \ln \left( \frac{P_{tyre}}{P_{recommended}} \right) \quad (15)$$

According to this equation, the maximum stress increases as tire pressure and wheel load increase, and decreases as it approaches the recommended pressure.

The contact area was calculated with the super ellipse model developed by Hallonborg and estimated using the contact width ( $w_A$ ) and contact length ( $l_A$ ) in this model [27]. The vertical stress distribution between the center and the edge of the contact area is modeled by Equation 17

$$A = kw_A l_A \quad (16)$$

$$\sigma_y = C \left( \frac{w(x)}{2} - y \right) e^{-\delta \left( \frac{w(x)}{2} - y \right)} \quad (17)$$

$$0 \leq y \leq \frac{w(x)}{2}$$

This equation is used to predict the stress distribution in the contact area and has been reported to give high agreement with the measured stress values.

The model was successful in predicting the stress distribution and soil compaction of agricultural tires, providing accurate results with practically accessible data. However, the validity of this model needs to be tested in different soil types and field conditions. Future studies should aim to expand this model and make it applicable in the field to more accurately predict the impacts of agricultural tires.

### 2.12. Effects of Stress Zones Caused by Agricultural Vehicles on Soil Structure

The pressure exerted by agricultural machinery on the soil causes soil compaction and deterioration of the pore structure. The pore system that provides water and air permeability of the soil shrinks as a result of compression, negatively affecting plant root development Berisso et al. [28] investigated the change in the stress effects of tires on the soil pore structure and carried out this study with four wheel passes in a clayey soil. A forage harvester with a width of 80 cm carrying a total load of 6100 kg was used and normal and horizontal stresses were measured with load cells. Pore continuity index and air-filled porosity degree were calculated using different air permeability values.

As a result of the study, it was found that air filling and air permeability were at the lowest level in the center of the tire track, while these values were higher outside the tire track. It has been determined that the pore structure in the center of the tire track is tighter and distorted due to pressure. On the short edges, pore continuity is disrupted but air permeability is preserved. The average normal stress was calculated using the internal pressure (PI) with the help of Equation 18 [29]:

$$\sigma_m = \frac{PI}{2(1-\nu_m)} \quad (18)$$

When the Poisson ratio ( $\nu_m$ ) is taken as 0.3, the  $\sigma_m$  value is found to be 40% more than the internal pressure. Air permeability ( $k_a$ ) was calculated using the height of the soil sample ( $l_s$ ), dynamic air viscosity ( $\eta$ ), air pressure difference ( $\Delta P$ ), cross-sectional area ( $A_s$ ) and volumetric flow rate ( $\phi$ ). These data show that the stresses exerted by tires on the soil significantly alter the pore structure and impede water/air circulation.

$$\sigma_m = \frac{PI}{1.4} \quad (19)$$

$$k_a = \frac{-\phi l_s \eta}{\Delta P A_s} \quad (20)$$

These studies have revealed that agricultural tires reduce the pore continuity index and lower air permeability. High pressure in the centre of the tire causes the pores to become less connected and the air transmission capacity to decrease. These findings highlight critical points to consider in the design and use of agricultural machinery and indicate the need for strategies aimed at preserving the pore structure. Future studies could investigate the long-term effects of different tire types and inflation pressures to develop recommendations for more sustainable agricultural practices.

### 2.13. Calculating Tire Footprint Area on Hard Ground

Grečenko [30] tried to calculate the tire footprint area on hard ground. Many existing formulas include load deformation as a parameter to calculate tire tread area. A user can only see the data of usage pressure, usage rim and the amount of load the tire can carry from the tire catalog. In his study, Grečenko [30] aimed to evaluate the tire tread area with arbitrary loading and inflation pressure, using existing formulas and a tire catalogue, suggesting the application of a specific correction factor. This provides an accurate estimate of the average contact pressure.

In the developed model, the track area ( $A_o$ ) was calculated using the tire track length ( $l_o$ ), track width ( $b_o$ ) and shape coefficient ( $k$ ) (Equation 21). The shape coefficient,  $k$ , defines the geometric shape of the wake field:  $k = \pi$  If , it indicates an ellipse, if  $\pi < k < 4$  it indicates an oval and if  $k=4$  it indicates a rectangular shape. The section height ( $h_k$ ) and total diameter ( $d_k$ ) of the tire are other basic parameters used in the equations. Nominal load deflection is the deformation of the tire under a certain load and is calculated using the static radius ( $r_s$ ) and rim diameter ( $d_r$ ). The nominal load deflection ( $f_{kj}$ ) is shown with the ratio ( $a$ ) symbols.

$$A_o = k \frac{l_o}{2} \frac{b_o}{2} \quad (21)$$

$$k = \frac{4A_{om}}{l_o b_o} \quad (22)$$

$$h_k = \frac{d_k - d_r}{2} \quad (23)$$

$$a = \frac{h_k}{b_k} = \frac{d_k - d_r}{2b_k} \quad (24)$$

$$f_{kj} = \frac{d_k - 2r_s}{2} \quad (25)$$

$$\frac{f_{kj}}{h_k} = \frac{d_k - 2r_s}{d_k - d_r} \quad (26)$$

This model accurately predicts tire footprints in hard ground conditions, providing engineers with better data for vehicle design and tire selection. Taking into account parameters such as percentage nominal deflection (Equation 26) and section width ( $b_k$ ) allows for more accurate prediction of tire footprint at different pressure-load combinations. However, further testing of experimental data on different ground conditions and load cases is required.

This approach proposed by Grecenko [30] provides an important model for accurately calculating tire footprint area, especially in hard ground conditions. The model can be used to assess the potential for soil compression and compaction of the tire track area. However, future studies could test the accuracy of this model in agricultural and variable ground conditions, providing more comprehensive data to optimize tire choices and soil conservation.

#### 2.14. Modelling of Stress and Compaction in Soil Caused by Agricultural Field Traffic

Soil compaction is the physical deterioration caused by the pressure applied to the soil by agricultural machinery, and this causes the soil pores to decrease, water and air permeability to decrease, thus negatively affecting plant growth. Keller and colleagues [31] conducted a modeling study to evaluate the effects of agricultural land traffic on soil and developed a model that estimates the stress and compression caused by the passage of agricultural machinery.

The developed SoilFlex model is a two-dimensional contact model and for using to calculate the tire-soil interaction. The contact area and contact stress are obtained from parameters such as tire load, inflation pressure and tire width and normal (vertical) stresses and shear (horizontal) stresses are examined separately. Soil properties such as soil density and volumetric strain are included in the parameters of this model. They used different methods in measuring volumetric stress in their studies. Three different methods were investigated for the calculation of soil density and volumetric stress: Larsson et al. [32], Bailey and Johnson [33], O'Sullivan and Robertson [34]. The stress distribution was calculated using the Boussinesq [19] and Cerruti [35] equations.

The SoilFlex model was able to successfully predict the stress distribution and displacement in the contact area due to tire load. The model was found to accurately predict stress distribution and compression effects when compared with real-world data. The study showed that the size and shape of the tire-soil contact area directly affects the depth and spread of soil compaction. Therefore, optimum tire inflation pressure and reduction of machine passes are important to minimise damage to the soil.

These modeling studies provide critical data to assess and minimize the negative impacts of agricultural activities on soil. However, these models need to be tested under different soil types and climatic conditions. Future work should focus on improving the prediction accuracy of the SoilFlex model under different soil conditions and machine loads. In addition, this model can be optimized in the design and usage processes of agricultural machinery through long-term field studies.

#### 2.15. Investigation of the Pressures Created by Tractor Tires on the Ground

The interface pressure of tractor drive tires on the soil is an important parameter affecting soil compaction and traction performance. Thomas and Kishimoto [2] investigated the interface pressures of different combinations of dynamic load and inflation pressure in clay and sandy soils using 18.4R38 radial-ply tires. In structured clay soil, the pressures on the tire tread surface were found to be higher than the inflation pressure, while the pressures under the tire tread were found to be lower. In loose sandy and clayey soils, the pressures were close to or below the inflation pressure. On different ground types, the tire tread area varied, which directly affected the pressure applied to the soil and the risk of compaction.

The research revealed that the tire footprint area was 10% wider in loose sandy soil and 4% wider in loose clay soil. As tire inflation pressure and load increased, the interface pressure in clay soil reached higher values on the tread surface, which increased the tendency for soil compaction. However, the effect of similar load and pressure changes on the interface pressure in loose soils was more limited.

Results show the effect of tractor tire pressure and load condition on soil compaction and traction performance. By optimizing inflation pressure, the efficiency of tractors can be increased and soil compaction can be minimized. However, more comprehensive studies conducted under different soil types and climate conditions could increase the accuracy of these findings in application in agriculture. A better understanding of the interaction mechanism with soil will contribute to the planning of more efficient and environmentally friendly agricultural activities.

## 2.16. Comparison of Soil Stresses Caused by Agricultural Machinery with Simulation Model

Keller and colleagues [36] conducted experiments under different soil types and loading conditions to measure and simulate the vertical stress effects of agricultural machinery on the soil. In the study, data obtained during wheel passes in five different soil types (13-66% clay content) were used and the results were compared with the Boussinesq and Frohlich solutions based on classical elasticity theory. The Boussinesq model describes the vertical stress distribution caused by a single normal force on the surface, while Frohlich added a "concentration factor" to this model and defined it from a broader perspective.

Boussinesq [19] developed a model to describe the normal stress distribution on a homogeneous isotropic elastic half-space surface due to a single normal force applied to a surface, and explained the vertical stress ( $\sigma_z$ ) on the surface with the following equation:

$$\sigma_z = \frac{3P z^3}{2\pi r^5} \quad (27)$$

$$r = (x^2 + y^2 + z^2)^{1/2}$$

Here,  $\sigma_z$  is the simulated vertical soil stress (Pa), P is the point load on the surface (N), z is the depth of the load (m) and r is the distance from the point of impact of the point load to the desired location (m). r the value is defined as the square root of the sum of the squares of the horizontal (x, y) and vertical (z) coordinates of the load point.

Frohlich [26] added a concentration factor (v) to this model to describe the stress distribution more broadly:

$$\sigma_z = \frac{vP z^v}{2\pi r^{v+2}} \quad (28)$$

Here, the coefficient v controls the intensity of the stress distribution and when v = 3, the equation agrees with Boussinesq's solution based on classical elasticity theory. This parameter affects the distribution of the load applied to the surface along the depth and the spread of the stress curves.

To evaluate the impact of agricultural machinery on the soil, each small element of the load in the tire-soil or track-soil contact area can be treated as point loads. In this case, the total stress is calculated by summing the stress values of all the small elements in the contact area of the surface load (Söhne 1953). In this approach, developed by Söhne and using similar principles, the total stress ( $\sigma_z$ ) is expressed as:

$$\sigma_z = \sum_{i=0}^n \frac{vP_i z_i^v}{2\pi r_i^{v+2}} \quad (29)$$

In this equation,  $P_i$  represents the point load (N) on each small point element,  $z_i^v$  represents the depth of this element (m),  $r_i^v$  represents the distance of the element from the point load to the desired location (m), and v represents the concentration factor. This formula summarizes how stress varies with depth and the effect of each point load at

different depths. Therefore, such models are used to understand how soil stresses under surface load change with depth and to minimize stress effects in the design of agricultural machinery.

In the simulations, each small area where the tire contacts the ground is treated as point loads and the vertical stress is estimated by calculating the sum of these loads. The vertical stress values measured with simulations based on the Boussinesq solution showed agreement above 90%. This high degree of agreement enabled accurate modeling of tire width, load and contact patch parameters.

The results showed that vertical stresses in elastic-plastic layered soils with weak upper layers were higher than in homogeneous soils, but this difference remained limited. Study recommends better modeling of tire-soil interactions and optimizing tire design parameters to minimize soil compaction by agricultural machinery.

This research shows that the effects of agricultural tires on soil can be reliably predicted by simulations and that such modeling studies can be an important guide in the design of agricultural machinery. However, the validity of the model needs to be tested under different soil types and more complex loading conditions. Future field tests can be used to increase the accuracy of these simulations and minimize the negative effects of agricultural machinery on soil structure.

### 2.17. Effect of Different Tire Load and Different Inflation Pressure on Soil Tension

Arvidsson and Keller [1] studied the effects of different tire loads (11, 15 and 33 kN) and inflation pressures (70, 100 and 150 kPa) on the stress distribution in the upper and lower soil layers. In the experiments, five stress sensors at 10 cm depth and sensors at 30, 50 and 70 cm depth were used to measure subsoil stresses. The data obtained showed that the maximum stress at 10 cm depth was 39% higher than the tire inflation pressure and that the stress increased with increasing tire load. In the subsoil, the effect of inflation pressure decreased, but tire load stood out as a determining factor on subsoil tension.

Vertical stresses ( $\sigma_z$ ) were calculated with the model developed by Söhne [37] and formulated based on the Boussinesq equations. Tire load and inflation pressure are the most important parameters affecting the pressure distribution applied to the soil surface. Söhne's model describes the stress distribution on the surface using the tire's load and contact area parameters with the following equation:

$$\sigma_z = \sum_{i=0}^n \frac{vP_i}{2\pi Z^2} \cos^{v+2} \theta_i \quad (30)$$

Here,  $\sigma_z$  is the vertical stress (kPa),  $P_i$  is the load of each point element (kN),  $Z$  is the depth (m),  $\theta$  is the angle between the point load vector and the position vector. The equation is used to calculate how the tire load and contact pressure change the stresses through the soil depth.

The study found that tire inflation pressure affects stress distribution in the topsoil, but this effect decreases in the subsoil and tire load plays a greater role. As the tire load increases, it has been observed that the stress values in the subsoil decrease linearly or parabolically from the center of the tire track to the edges. The results show that tire load and inflation pressure should be carefully optimised to reduce the risk of soil compaction.

This study highlights that tire load and inflation pressure are of great importance to correctly understand and minimize the impacts of agricultural machinery on the soil. While the inflation pressure is decisive in the topsoil, the effect of the load is more critical in the subsoil. Future field studies can test the validity of these models under different soil types and loading conditions, helping develop strategies to increase long-term agricultural productivity and prevent soil compaction.

## 3. CONCLUSIONS

In this review, the effects of agricultural tire technologies on soil compaction, traction performance and agricultural productivity in agricultural activities were comprehensively investigated. Findings from the literature reveal that new



generation tires with low inflation pressure significantly reduce soil compaction by providing a large contact area. The use of such tires has the potential to reduce soil compaction and damage, while also increasing agricultural productivity. Findings show that low inflation pressure tires create a large contact area in agricultural activities, spreading the stress distribution more evenly and thus providing favorable conditions for plant root development [3, 6]. Moreover, it has been determined that optimum tire design and inflation pressure setting improves tractor performance by increasing traction and energy efficiency. Notably, radial tires exhibit a higher deflection capacity compared to bias tires, which makes them more effective at preventing soil compaction [13]. The ballast effect stands out as a critical factor in controlling soil compaction and increasing net traction power. The use of ballast provides an effective solution for preserving soil fertility by providing a more balanced load distribution, especially in radial tires.

Findings based on modeling studies highlight that accurately simulating tire and soil interactions plays an important role in planning agricultural activities and increasing productivity. Simulations have shown that the effects of tires on soil can be reliably predicted under different inflation pressures and soil conditions [21, 25]. However, existing models need to be tested with larger data sets under field conditions. Future modelling studies should be expanded to increase the accuracy of predictions for more complex soil structures and variable climatic conditions.

This review demonstrates that appropriate tire selection and use is critical to ensuring the sustainability of agricultural operations. In particular, the use of low inflation pressure tires creates a large contact area, increasing agricultural productivity and preserving the long-term health of the soil. As a result, it is recommended that tire load, inflation pressure and ballast applications be carefully optimized to minimize the negative impacts of agricultural machinery on the soil and ensure efficient use of the soil.

In future studies, testing the potential of new generation tire designs to increase energy efficiency and reduce soil compaction in agricultural machinery is thought to provide significant progress in agricultural machinery technologies. In this regard, in addition to field studies, the development of advanced modeling methods that can more accurately simulate soil compaction and traction force is also of great importance.

## ORCID

Onur KARAÇAY  <https://orcid.org/0000-0002-3650-816X>

Süleyman KILIÇ  <https://orcid.org/0000-0002-1681-9403>

## CONFLICT OF INTEREST

The authors declare that this study has no financial or commercial relationship with any organization or people working with them.

## REFERENCES

- [1]. Arvidsson J, Keller T. (2007). Soil stress as affected by wheel load and tyre inflation pressure. *Soil and Tillage Research*. 96(1):284-91 <https://doi.org/10.1016/j.still.2007.06.012>
- [2]. Way TR, Kishimoto T. (2004). Interface Pressures of a Tractor Drive Tyre on Structured and Loose Soils. *Biosystems Engineering*. 87(3):375-86. <https://doi.org/10.1016/j.biosystemseng.2003.12.001>
- [3]. ten Damme L, Stettler M, Pinet F, Vervaet P, Keller T, Munkholm LJ, et al. (2020) Construction of modern wide, low-inflation pressure tyres per se does not affect soil stress. *Soil and Tillage Research*. 204:104708. <https://doi.org/10.1016/j.still.2020.104708>
- [4]. Janulevičius A, Damanauskas V. (2022). Prediction of tractor drive tire slippage under different inflation pressures. *Journal of Terramechanics*. 101:23-31. <https://doi.org/10.1016/j.jterra.2022.03.001>
- [5]. Keller T. (2005). A model for the prediction of the contact area and the distribution of vertical stress below agricultural tyres from readily available tyre parameters. *Biosystems engineering*. 92(1):85-96. <https://doi.org/10.1016/j.biosystemseng.2005.05.012>
- [6]. Rodríguez LA, Valencia JJ, Urbano JA. (2012). Soil compaction and tires for harvesting and transporting sugarcane. *Journal of Terramechanics*. 49(3):183-189. <https://doi.org/10.1016/j.jterra.2012.04.002>
- [7]. Karaçay O, Kılıç S. (2024). Traktör Uygulamalarında Kullanılan Standart Yapı ve IF Lastik Yapısına Sahip Lastiklerin Taban İzlerinin ve Sehim Değerlerinin Kıyaslanması. *Karaelmas Fen ve Mühendislik Dergisi*.14(2):111-118.

- [8]. Harris BJ. Increased Deflection Agricultural Radial Tires Following the Tire and Rim Association IF, VF, and IF/CFO Load and Inflation Standards. (2017). <https://elibrary.asabe.org/data/pdf/6/913c0117/913C0117.pdf>
- [9]. Shaheb MR, Venkatesh R, Shearer SA. (2021). A Review on the Effect of Soil Compaction and its Management for Sustainable Crop Production. *Journal of Biosystems Engineering*. 46(4):417-439. <https://doi.org/10.1007/s42853-021-00117-7>
- [10]. Michelin. Lastik Teknolojisi.(2024). [Available from: <https://pro.michelin.com.tr/lastik>]
- [11].Renius K. CIGR. (1999).Handbook of Agricultural Engineering, Volume III Plant Production Engineering, Chapter 1 Machines for Crop Production, Parts 1.1. 27-1.1. 33 Tractors: Two Axle Tractors. <https://doi.org/10.13031/2013.36342>
- [12].Maclaurin B. (2014).Using a modified version of the Magic Formula to describe the traction/slip relationships of tyres in soft cohesive soils. *Journal of Terramechanics*.52:1-7. <https://doi.org/10.1016/j.jterra.2013.11.005>
- [13].Kumar S, Pandey KP, Kumar R, Ashok Kumar A. (2018). Effect of ballasting on performance characteristics of bias and radial ply tyres with zero sinkage. *Measurement*. 121:218-224. <https://doi.org/10.1016/j.measurement.2018.02.043>
- [14].Cokertire. Bias Ply or Radial | What is the Right Choice for Your Collector Car? (2024). [Available from: <https://www.cokertire.com/bias-ply-radial>]
- [15].Komandi G. (1976). The determination of the deflection, contact area, dimensions, and load carrying capacity for driven pneumatic tires operating on concrete pavement. *Journal of Terramechanics*. 13(1):15-20. [https://doi.org/10.1016/0022-4898\(76\)90028-8](https://doi.org/10.1016/0022-4898(76)90028-8)
- [16].Komandi G. (1990). Establishment of soil-mechanical parameters which determine traction on deforming soil. *Journal of Terramechanics*. 27(2):115-124. [https://doi.org/10.1016/0022-4898\(90\)90004-6](https://doi.org/10.1016/0022-4898(90)90004-6)
- [17].ten Damme L, Stettler M, Pinet F, Vervaet P, Keller T, Munkholm LJ, et al. (1990). The contribution of tyre evolution to the reduction of soil compaction risks. *Soil and Tillage Research*. 194:104283. <https://doi.org/10.1016/j.still.2019.05.029>
- [18].Eggers C, Berli M, Accorsi M, Or D. (2006). Deformation and permeability of aggregated soft earth materials. *Journal of Geophysical Research: Solid Earth*. 111(B10). <https://doi.org/10.1029/2005JB004123>
- [19].Boussinesq J. (1885). Application des potentiels à l'étude de l'équilibre et du mouvement des solides élastiques: principalement au calcul des déformations et des pressions que produisent, dans ces solides, des efforts quelconques exercés sur une petite partie de leur surface ou de leur intérieur; mémoire suivi de notes étendues sur divers points de physique mathématique et d'analyse: Gauthier-Villars.
- [20].Das BM, Sobhan K. (1990). Principles of geotechnical engineering.
- [21].Oh J, Nam J-S, Kim S, Park Y-J. (2019). Influence of tire inflation pressure on the estimation of rating cone index using wheel sinkage. *Journal of Terramechanics*. 84:13-20.
- [22].Misiewicz PA, Richards TE, Blackburn K, Godwin RJ. (2016). Comparison of methods for estimating the carcass stiffness of agricultural tyres on hard surfaces. *Biosystems Engineering*. 147:183-192. <https://doi.org/10.1016/j.biosystemseng.2016.03.001>
- [23].Arvidsson J, Westlin H, Keller T, (2011).Gilbertsson M. Rubber track systems for conventional tractors–Effects on soil compaction and traction. *Soil and Tillage Research*. 117:103-109. <https://doi.org/10.1016/j.still.2011.09.004>
- [24].People's Republic of China, from <https://tr.made-in-china.com>, accessed on 2024-10-01
- [25].Jjagwe P, Tekeste MZ, Alkhalifa N, Way TR. (2023). Modeling tire-soil compression resistance on artificial soil using the scaling law of pressure-soil sinkage relationship. *Journal of Terramechanics*. 108:7-19. <https://doi.org/10.1016/j.jterra.2023.02.002>
- [26].Fröhlich OK. (1934). Druckverteilung im Baugrunde: mit besonderer Berücksichtigung der plastischen Erscheinungen. Springer.
- [27].Hallonborg U. (1996).Super ellipse as tyre-ground contact area. *Journal of Terramechanics*. 33(3):125-132. [https://doi.org/10.1016/S0022-4898\(96\)00013-4](https://doi.org/10.1016/S0022-4898(96)00013-4)
- [28].Berisso FE, Schjønning P, Lamandé M, Weisskopf P, Stettler M, Keller T. (2013). Effects of the stress field induced by a running tyre on the soil pore system. *Soil and Tillage Research*. 131:36-46. <https://doi.org/10.1016/j.still.2013.03.005>
- [29].Berli M, Eggers C, Accorsi M, Or D. (2006). Theoretical analysis of fluid inclusions for in situ soil stress and deformation measurements. *Soil Science Society of America Journal*. 70(5):1441-1452. <https://doi.org/10.2136/sssaj2005.0171>

- [30]. Grečenko A. (1995). Tyre footprint area on hard ground computed from catalogue values. *Journal of Terramechanics*. 32(6):325-333. [https://doi.org/10.1016/0022-4898\(96\)00003-1](https://doi.org/10.1016/0022-4898(96)00003-1)
- [31]. Keller T, Défossez P, Weisskopf P, Arvidsson J, Richard G. (2021). SoilFlex: A model for prediction of soil stresses and soil compaction due to agricultural field traffic including a synthesis of analytical approaches. *Soil and Tillage Research*. 93(2):391-411. <https://doi.org/10.1016/j.still.2006.05.012>
- [32]. Larson W, Gupta S, Useche R. (1980). Compression of agricultural soils from eight soil orders. *Soil Science Society of America Journal*. 44(3):450-457. <https://doi.org/10.2136/sssaj1980.03615995004400030002x>
- [33]. Bailey A, Johnson C. (1988). A soil compaction model for cylindrical stress states. <https://www.cabidigitallibrary.org/doi/full/10.5555/19892439345>
- [34]. O'Sullivan M, Robertson E. (1996). Critical state parameters from intact samples of two agricultural topsoils. *Soil and Tillage Research*. 39(3-4):161-173. [https://doi.org/10.1016/S0167-1987\(96\)01068-9](https://doi.org/10.1016/S0167-1987(96)01068-9)
- [35]. Cerruti V. (1893). Sulla deformazione di un corpo elastico isotropo per alcune speciali condizioni ai limiti. *Il Nuovo Cimento* (1877-1894). 34(1):115-24. <https://doi.org/10.1007/BF02709665>
- [36]. Keller T, Berli M, Ruiz S, Lamandé M, Arvidsson J, Schjønnig P, et al. (2014). Transmission of vertical soil stress under agricultural tyres: Comparing measurements with simulations. *Soil and Tillage Research*. 140:106-17. <https://doi.org/10.1016/j.still.2014.03.001>
- [37]. Söhne W. (1953). Druckverteilung im boden und bodenverformung unter schlepperreifen. *Grundlagen der Landtechnik-Konstrukteurhefte*. (5): 49-63.

---

*Techno-Science Paper ID: 1563596*

# A Healthcare Monitoring System Design for Elderly Living Alone

Ozlem COSKUN<sup>1\*</sup> 

<sup>1</sup> Department of Electrical and Electronics Engineering, Suleyman Demirel University

## ABSTRACT

Due to advancements in the field of medicine, the elderly population has significantly increased around the world. Since the young population is also working, elderly people are left alone at home. Problems such as Alzheimer's, sleepwalking, and decreased mobility in these elderly individuals living alone reduce the quality of life of both individuals and their families. This study aims to develop a specialized tracking system to address issues faced by elderly individuals, such as getting lost while living alone. Nowadays, thanks to GPS technology, it is possible to monitor individuals easily even from our phones. It will be easier to monitor places in the house where there is a high probability of falling and by using an infrared sensor to control the entrances and exits of the house. It is clearly seen that older people prefer simple rather than complex technological products when using them. For this reason, a design has been made that will be sufficient to carry with you without having to make any adjustments in the mobile application.

**Keywords:** Smart healthcare, Telemedicine, GPS, Elderly tracking

## 1. INTRODUCTION

Health technologies are one of the most important needs in human life. Today, the use of mobile applications in any field and the desire of people who always want to be online affect and change the development of technologies in all sectors, as well as in the health sector. With technological advancements, it is now possible to create a low-cost home healthcare monitoring system that captures bodily signals, visualizes them, and transmits them remotely. With the increase in mobile applications, patient monitoring is becoming easier. In this context, with the mobile patient monitoring system; There is no need to go to the hospital for basic measurements and continuous monitoring [1,2,3,4]. According to the World Health Organization, telemedicine; improving the health of individuals and societies, preventing diseases and accidents; It is defined as the provision of health services by all health professionals using information and communication technologies, remotely and with valid information communication methods, with the continuous training of health personnel [5,6].

Determining the location has always been an important technology for humankind. In ancient times, this was roughly determined by natural resources such as trees, mountains, stars, sun and moon. In parallel with the advancement of technology, ground stations have begun to be established [7]. However, the failure of these systems to fully meet the needs has led to new searches and allowed the development of satellite-based positioning systems used today. The widespread use of GPS technology and its ability to provide location almost without error has paved the way for the widespread use of tracking systems. The expectation of relatives of the elderly is to instantly determine the location of those they are responsible for. With today's technology, determined location information can be transmitted to a remote center via mobile communication systems.

GSM-based GPRS technology is one of the most commonly used systems for this purpose. Mobile communication systems can be used without a fixed point, offering ease of communication, time-saving benefits, and spatial independence [8]. This technology facilitates locating and responding to sick, disabled, or elderly individuals who wander from home in emergency situations. With the help of infrared sensors and NodeMCU, entrances and exits

\*Corresponding Author Email: [ozlemcoskun@sdu.edu.tr](mailto:ozlemcoskun@sdu.edu.tr)

Submitted: 19.09.2024 Revision Requested: 07.10.2024 Last Revision Received: 22.10.2024

Accepted: 05.11.2024 Published Online: 26.11.2024



Burdur  
Mehmet Akif Ersoy  
University Press



Cite this article as: Coşkun, Ö. (2024). A Healthcare Monitoring System for Elderly Living Alone.

Scientific Journal of Mehmet Akif Ersoy University, 7(2): 81-90.

DOI: <https://doi.org/10.70030/simakeu.1552983>

<https://dergipark.org.tr/simakeu>



Content of this journal is licensed under a Creative Commons Attribution-NonCommercial 4.0 International License.

from the house are kept under control. The widespread use of NodeMCU and infrared sensors also provides an advantage in terms of supply and reduced costs.

## 2. LITERATURE REVIEW

Health monitoring systems have started to increase rapidly recently. Different smart systems are being designed to monitor the current health status of patients. In a study [9], a system using GSM/GPS technologies is proposed to control the patient's blood pressure and body temperature. This system offers an intelligent, real-time health monitoring and tracking system. In case of emergency, the values found via the GSM module will be sent via text message to the doctor's mobile phone number. In addition, GPS will allow location information to be given to the patient who is desired to be kept under constant observation.

One of the new developments in the healthcare sector is patient monitoring systems based on remote monitoring of patients, which have many advantages against the problems of increasing health problems and the rapidly aging world population. It is sufficient to choose simpler applications for monitoring patients in healthcare institutions. Technology has advanced enough to allow the patient to be monitored even while performing their daily activities at home, with the use of modern communication and sensor technologies. Sensors are available today to monitor basic vital signs such as electrocardiogram reading, heart rate, respiratory rate, blood pressure, temperature, blood sugar levels, and nervous system activity. The range of remote healthcare services has a wide range of uses, from chronic patients, the elderly, premature children and accident victims. Thanks to new technologies, patients can be monitored based on disease or condition. The technology ranges from body-worn sensors to ambient sensors attached to the environment, with new studies aiming for non-contact monitoring that only requires the patient to be a few meters away from the sensor. Fall detection systems and applications for monitoring chronic patients are already in use [10,11].

P. Varady and colleagues introduce an innovative approach to patient monitoring in their work [12]. With this approach, a patient tracking application was built based on an existing industry standard communication network created using standard hardware tools and software technologies. Thanks to this patient monitoring application, open architecture system modeling, scalability, standard interfaces and flexible signal interpretation opportunities are offered.

In their study, Mohammad Salah and his colleagues [13] proposed an intelligent patient monitoring system to automatically monitor the health status of patients through connected networks based on sensors. Various sensors are used to collect the patient's biological behavior. The important biological information obtained from the sensors is then sent to the IoT cloud. The system is a patient monitoring system that can detect the critical condition of a patient by processing sensor data and provide instant notification to doctors/nurses and hospital responsible staff. In addition, patient relatives can also benefit from this system with limited access.

## 3. PART OF HEALTHCARE MONITORING SYSTEMS

### 3.1. GPS Module

Global Positioning System is a system that uses the 1.5 GHz band and enables the determination of the exact location (with a margin of error of 5m) thanks to the satellite network that operates continuously around the world [8]. In order to determine its own position, the GPS receiver must know the exact location of the satellites and its distance to the satellites. The basic measure to determine the distance to satellites is the travel time of the signal between the satellite and receiver antennas. The distance to the satellite is equal to the arrival time of the sent signal multiplied by its speed. The arrival time is included in the coded signals coming from the satellites. The GPS receiver tries to match the code it produces with the code coming from the satellite. By comparing these two codes, it detects the delay. Multiplying this delay with the speed of light gives the distance to the satellites. Different measurement methods are applied in GPS depending on the type of points measured, the desired sensitivity and the purpose. The coordinates obtained as a result of the measurement vary depending on the receiver type, observation period,

location and number of satellites, and measurement type. If the point to be determined is stationary, static position determination; If it is mobile, we are talking about dynamic positioning. The basic parts of GPS are given in Fig 1.

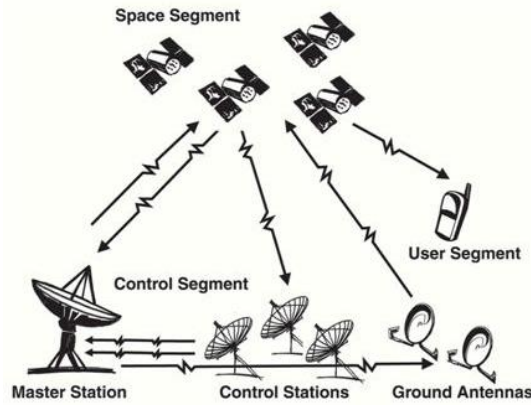


**Fig 1.** Basic working mechanics of GPS

NEO-6M module is used for location control and tracking using GPS. This module has many connection options. The 50-channel u-blox 6 positioning engine offers first correction time under one second. Thanks to the 3V-5V converter unit, it can be interfaced with 5V Microcontrollers. It consists of four pins: 5V, TX, RX and GND. There is no need for external components in this independent 5V GPS module.



**Fig. 2.** NEO-6M GPS module

### 3.2. PIR Sensors

PIR sensors are electronic sensors that detect presence and movement in the environment. PIR sensors detect differences in the rate of IR-infrared radiation that vary depending on the temperature and surface properties of objects in front of the sensor. When a person passes in front of a background, such as an object or a wall, the temperature at that point in the sensor's view changes from room temperature to body temperature and then back to its initial state. The sensor converts the resulting change in incoming infrared radiation into a change in output voltage and this triggers detection. The PIR sensor has a detection range, ranging from 2-3 meters. The PIR sensor back view is as shown in Fig.3 [14].

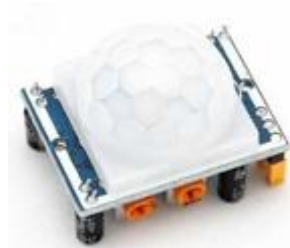


**Fig 3.** PIR sensor

### 3.3. Wi-Fi

The WLAN standard operating in the 2.4 GHz ISM band has become a popular positioning technology in corporate and public organizations in recent years. Since Wi-Fi signals, whose frequency and wavelength are given in Fig 3, are located in most buildings and are available on almost every mobile device, the demand for positioning systems with Wi-Fi signals is increasing day by day. Coverage range between 50 m and 100 m and 11, IEEE 802.11, a standard with a bit rate of 54 or 108 Mbps, is the standard that dominates local wireless networking today. Therefore, using the existing WLAN infrastructure by adding a location server for positioning has become attractive for individual and commercial positioning systems [15].

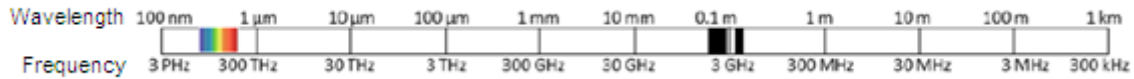


Fig 4. Wavelength and frequency range of Wi-Fi signals

### 3.4. Microprocessor Unit NodeMcu ESP8266

NodeMCU ESP8266 development board V3-CH340 Chip LoLin is a development board that contains an ESP8266 WiFi module with NodeMCU firmware installed on it. Since it was developed using the ESP8266 SDK, it supports GPIO, PWM, IIC, 1-Wire and ADC connections without the need for an extra microcontroller. It is affordable and breadboard compatible. This product can be used alone. Additionally, it does not require an arduino-like development board [16].



Fig 5. NodeMCU ESP8266 module

### 3.5. PHP

PHP is a general-purpose scripting language designed to create dynamic web pages. PHP codes are placed in HTML and interpreted with the PHP interpreter on the server to create the desired document. PHP is supported by many modern web servers and operating systems [17]. The PHP part that manages the server consists of two files. These are defined with the names "sendLocation.php" and "getLocation.php". With the sendLocation.php file, it saves the location information from the android program that sends data to the database. With the getLocation.php file, it sends the data in the database as output when a request comes to the android program that provides data tracking.

### 3.6. Telegram

Telegram is a multi-platform, secure instant messaging service. Telegram clients are available for both mobile (Android, iOS) and desktop systems (Windows, Linux). Thanks to location sharing and channels (bots), data sharing and matching with servers in various parts of the world can be done very quickly.

### 3.7. App Inventor

App Inventor is a free web application created by Google and later developed by the Massachusetts Institute of Technology (MIT). It allows beginners to easily create Android applications. It can be applied easily, especially thanks to its puzzle-like structure and drag-and-drop mechanism.

## 4. SYSTEM IMPLEMENTATION

### 4.1. Location Tracking

The location tracking design consists of two modules. One of the modules takes the coordinate data from the person to be monitored and updates the database on the server at regular intervals.

#### 4.1.1. Send Location

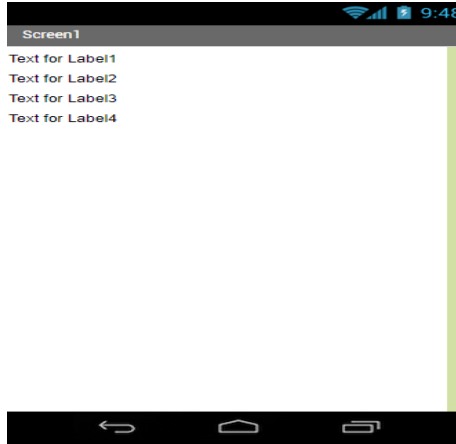


Fig 6. Main screen of the program

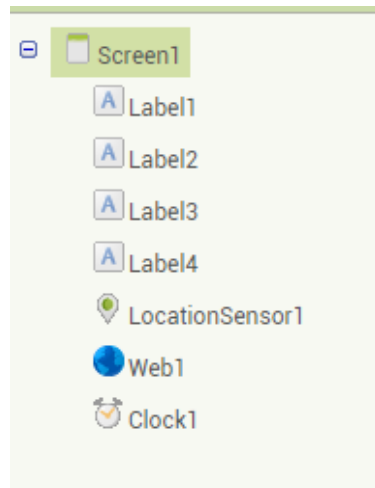
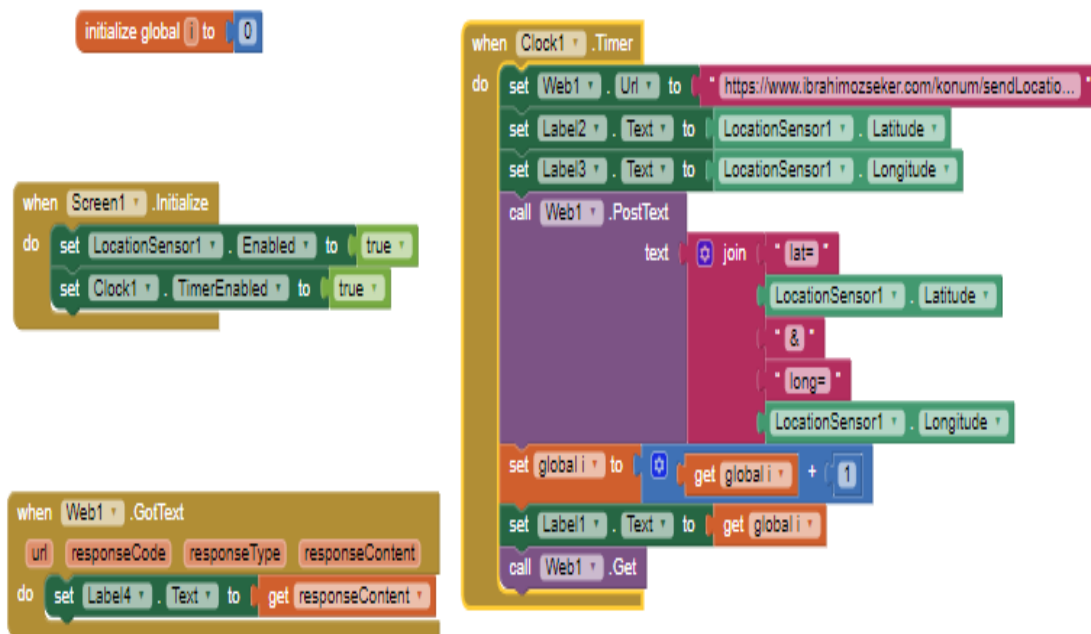


Fig 7. Components for creating the main screen of the program

As seen in Fig 7, the data sending module uses four labels, the phone's location sensor, a web module to send data to the server, and a clock module to perform this operation at regular intervals.





**Fig 8.** Block diagram used for the program to send location

As seen in Fig 8, when the program first runs, the position sensor and clock module are activated. In order for the clock module's processing time to operate accurately and stably, the database on the server is updated every second by taking coordinate data from the position sensor. Meanwhile, data from the database, which is also shown on the labels on the main screen, is printed on the screen.

### 4.1.2. Positioning

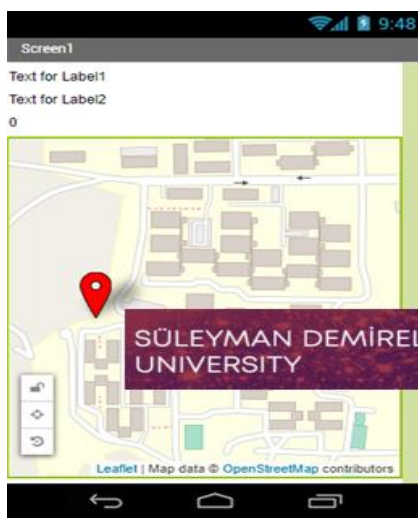


**Fig 9.** Main screen display with monitoring

Three tags were used in the program used for monitoring. The map module from these tags was used to show exact time location. Apart from this, clock and web modules have also been activated.

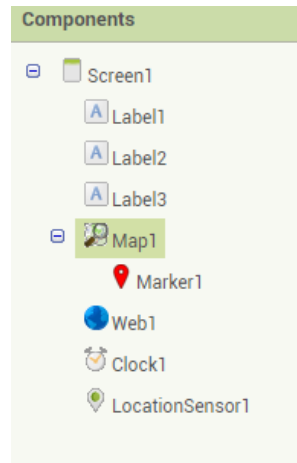


**Fig 10.** Components used for positioning

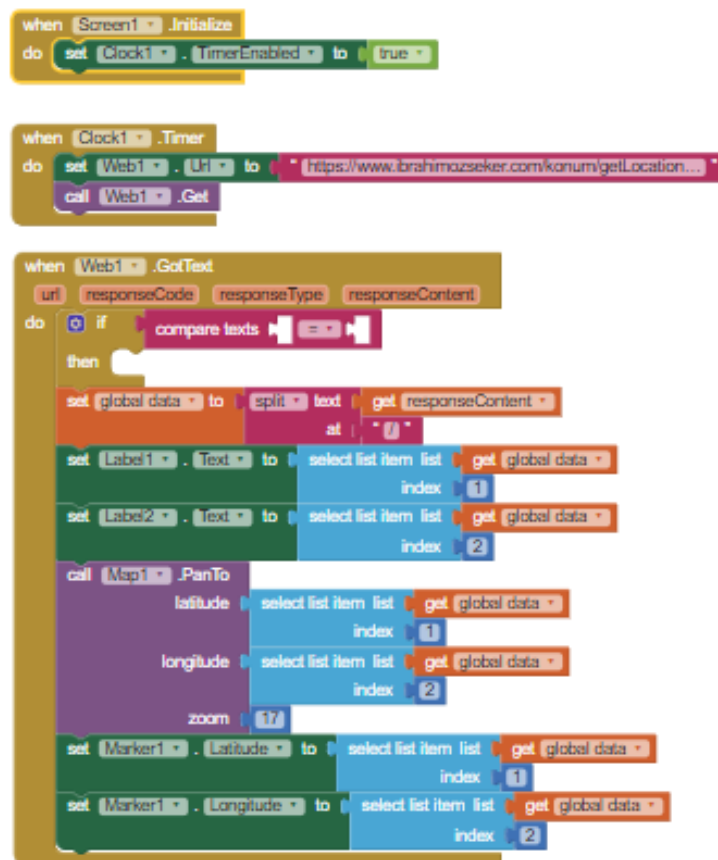


**Fig 11.** Block diagram used to position the program

When the program first runs, the clock module is activated and the update time is set to one second. Location information is received from the server every second. When this process is completed successfully, the location point on the map is updated according to the latest data and the process is completed.

**4.1.3. MySQL Database**

+ Options		id	lat	lon	ok
<input type="checkbox"/>	Arrangement	1	0	0	1

**Fig 12.** Table used for communication between programs

## 4. 2. Proposed In-Home Tracking System

### 4.2.1. Setting Up Telegram

A channel has been created on Telegram for broadcasting. A bot with web access was created in this channel, allowing it to broadcast to the user via Telegram.

### 4.2.2. Operation of the System

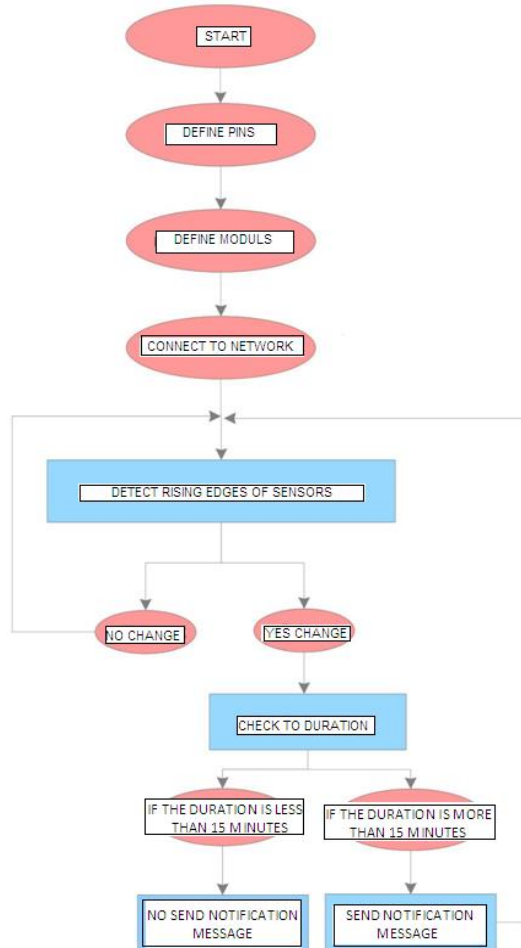


**Fig 13.** Operating block diagram of the system

When the program first runs, it connects to the Wi-Fi network and assigns itself an IP. Digital data from PIR sensors is read in a fixed loop, and while the digital data is being read, the rising edge is captured and the message of the active room is sent as a notification to the channel via the telegram bot. At the same time, a period of inactivity is started. If the time has already started, it is checked during the cycle whether it is less than the previously determined time. If the time has exceeded the specified time, the bot will send a message via the telegram channel notifying you of this.

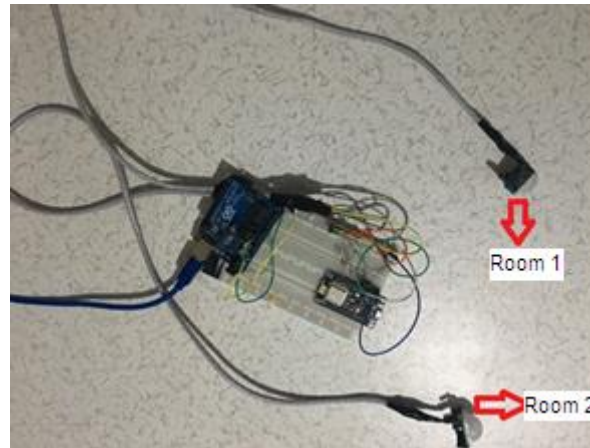


**Fig 14.** Completed in-home tracking system

In the design shown in Fig 14, when PIR sensors detect movement, they send notifications to telegram with their given names. While “Room 1” represents the bathroom/toilet, “Room 2” represents the outer door. When the time set in Room 1 (15 minutes) passes, the "there may be an emergency situation" notification is displayed; in Room 2, when you exit the outside door, the notification "leaving the house has been made" appears.

## 5. CONCLUSIONS

The aim of this study is to facilitate the follow-up of elderly individuals experiencing health problems. For this reason, the target audience of the project is considered to be older individuals living alone and disabled people. In this design, PIR sensors are planned to be placed in every room in a house, allowing complete individual tracking. With the help of these sensors, it is possible to track the elderly person by learning which rooms he stays in and for what periods of time. Their messages will come from the mobile application and if they are away from home, the patient's relatives will be able to follow up from the mobile application. This aims to prevent unwanted accidents.

Thanks to the use of this design, it is aimed to increase the quality of life of the users with ease and low costs. Considering the changing country conditions, individualism and loneliness are seen as the biggest problems of people in the future, especially lonely older people. Thanks to this technology, people's quality of life increases, the patient's range of motion increases, it provides real-time monitoring and increases the chance of early intervention. Despite the continuous studies and developing technology in this field, we have not reached a level where all the requirements are met. For this system to work error-free, high data transfer rate, reliable communication, and multiple and mobile receivers are needed.

## ORCID


Ozlem COSKUN  <https://orcid.org/0000-0001-8800-4433>

## REFERENCES

- [1]. Gogate, U., Bakal, J. (2018). Healthcare monitoring system based on wireless sensor network for cardiac patients. *Biomedical and Pharmacology Journal*, vol. 11, no. 3.pp. 1681–1688.
- [2]. Rotariu, C., Costin, H., Andrusac, G., Ciobotariu, R., Adochiei, F. (2011). An integrated system for wireless monitoring of chronic patients and elderly people. In *15th International Conference on System Theory, Control and Computing*, pp. 1–4.
- [3]. Sundara, B., Sarvepalli, K. C., Davuluri, S. H. (2013). GSM Based patient monitoring system in NICU. *IJRET Int. J. Res. Eng. Technolgy*, vol. 2, no. 07., pp. 120-123
- [4]. Chenhui, Z., Huilong, D., Xudong, L. (2008). An integration approach of healthcare information system. *International Conference of BioMedical Engineering and Informatics (BMEI 2008)*, pp.606-609.
- [5]. Sanli, M. (2009). Mobile patient tracking system. Master's Thesis, Kocaeli University Institute of Science and Technology.

- [6]. Yilmaz, A., Guven, A. (2017). Wireless patient monitoring system. *Electronic Letters on Science and Engineering*, 13(1), pp. 16-30.
- [7]. Derelioglu, B. (2007). GPS and GPRS based wide area network application. Master's Thesis Gazi University Institute of Science and Technology.
- [8]. Karaali, C., Yıldırım, O. (1996). Global positioning system (GPS). *Pamukkale University Faculty of Engineering Journal of Engineering Sciences*, Issue: 2, pp.103-108.
- [9]. Aziz, K., Tarapiah, S., Ismail, S. H., Atalla, S. (2016). Smart real-time healthcare monitoring and tracking system using GSM/GPS technologies. *Proceedings of the 2016 3rd MEC International Conference on Big Data and Smart City (ICBDSC)*, pp. 1–7.
- [10].Greene, S., Thapliyal, H., Carpenter, D. (2016). IoT-based fall detection for smart home environments. *IEEE International Symposium on Nanoelectronic and Information Systems*, pp. 23-28.
- [11].Luo, X., Liu, T., Liu, J., Guo, X., Wang, G. (2012). Design and implementation of a distributed fall detection system based on wireless sensor networks. *EURASIP Journal on Wireless Communications and Networking*, (1), 1-13.
- [12].Varady, P., Benyó, Z., Benyó, B. (2002). An open architecture patient monitoring system using standard technologies. *IEEE Transactions on Information Technology in Biomedicine*, 6(1), 95-98.
- [13].Uddin, M. S., Alam, J. B., & Banu, S. (2017). Real time patient monitoring system based on internet of things. *4th International Conference on Advances in Electrical Engineering (ICAEE)*, pp. 516-521.
- [14].Yavuz, S. O., Taşbaşı, A., Evirgen, A., Kara, A. (2012). Motion detector with PIR sensor usage areas and advantages. *Istanbul Aydın University Journal (İAÜD)*, Issue 14, pp. 7-16.
- [15].Belakbir, A., Amghar, M., El Kouhen, N. (2012). An indoor positionning system based on the fusion of location information. *Colloquium in Information Science and Technology (CIST)*, pp. 32-37.
- [16].Malik, A., Magar, A. M., Verma, H., Singh, M., Sagar, P (2019). A detailed study of an internet of things (IoT). *International Journal of Scientific & Technology Research* Volume 8, Issue 12. pp. 2989-2914.
- [17].Yilmaz, S., Sazak, B.S., and Cetin, S. (2010). Design and implementation of web-based training tool for a single switch induction cooking system using PHP. *Electronics and Electrical Engineering*. No. 3 (99).

# Wideband Microstrip Patch Antenna Design At 2.4 Ghz Frequency for Wireless Communication

Ozlem COSKUN<sup>1\*</sup> , Nazlihan ERGINYUREK<sup>1</sup> ,

<sup>1</sup> Department of Electrical and Electronics Engineering, Suleyman Demirel University

## ABSTRACT

The ever-increasing development of wireless and mobile communications, along with the rising volume of data and data traffic in wireless networks, requires these communications to be fast and uninterrupted. This can be achieved through the development of antennas with low return loss, high bandwidth, and compact size. In this study, an antenna design operating at a 2.4 GHz frequency was created using the CST Microwave Studio program to meet the need for broadband microstrip patch antenna designs. FR-4 material, which is 1.6 mm high, has a dielectric constant of 4.3 and a rectangular geometry with a loss tangent of 0.019, was used as the substrate material. At a resonance frequency of 2.4 GHz, the antenna was found to have a maximum gain of 2.27 dB and a maximum directivity of 7.28 dB in the same direction. Selection of new microstrip patch antenna configurations and development of accurate and versatile analytical models are of great importance in wireless communication technology.

**Keywords:** Patch antennas, CST Microwave studio, Reflection coefficient, Antenna gain

## 1. INTRODUCTION

In general, the transportation of information or a message produced by a source between two specific points through a channel is called communication. Microwave antennas hold the most significant role in today's wireless communication systems. The microstrip antenna concept, which gained significant popularity among microwave antenna types with its high performance, ease of installation, lightness and cheap manufacturing, was first put forward by Deschamps in 1953. Later, Gutton and Baissinot patented a microstrip antenna [1].

Microstrip patch antennas are integral components of wireless systems, and numerous techniques have been developed over the past three decades to increase their bandwidth. These techniques may include frequency-selective surface impedance matching networks, parasitic or multiple resonators, modification geometry of the radiating element, and the use of a substrate with a low dielectric constant or an increase in the thickness of the substrate. The purpose of the microstrip patch antenna is to radiate and receive electromagnetic energy in the microwave range. The operation and performance of a microstrip patch antenna are based on the geometry of the printed patch and the material properties of the substrate on which the antenna is printed [2,3].

Despite this, twenty years passed until photoetching techniques usable thermal and mechanical properties, and low loss rates were developed for a copper or gold-coated substrate with a wide range of dielectric constants, and practical antennas as good as their theoretical models were produced. This was mainly due to the lack of good dielectric bases available. With the development of these bases, microstrip antennas have also undergone rapid development. The first practical antennas were developed by Howel and Munson in the early 1970s. Since then, research and development have been carried out using microstrip antennas' numerous advantages such as lightness, small volume, cheapness, superficial appearance, and suitability for printed circuits; In the broad field of microwave antennas, microstrip patch antennas have pioneered a separate branch and led to various applications [4]. The popularity of microstrip antennas increased after 1970. In the following 1980s, the foundations of the production processes of microstrip antennas were laid [5].

\*Corresponding Author Email: [ozlemcoskun@sdu.edu.tr](mailto:ozlemcoskun@sdu.edu.tr)

Submitted: 19.09.2024 Revision Requested: 06.10.2024 Last Revision Received: 22.10.2024

Accepted: 05.11.2024 Published Online: 26.11.2024



Burdur  
Mehmet Akif Ersoy  
University Press



Cite this article as: Coşkun, Ö., Erginyürek, N. (2024). Wideband Microstrip Patch Antenna Design at 2.4 Ghz Frequency for Wireless Communication. Scientific Journal of Mehmet Akif Ersoy University, 7(2): 91-98.

DOI: <https://doi.org/10.70030/simakeu.1185245>

<https://dergipark.org.tr/simakeu>



Content of this journal is licensed under a Creative Commons Attribution-NonCommercial 4.0 International License.

## 2. MICROSTRIPS ANTENNAS

Microstrip antennas have been frequently used and become widespread, especially in recent years, in mobile communication systems, radar, aircraft, missile satellite and navigation fields. Rectangular H, E shaped, circular etc. Microstrip antennas with different geometric shapes are used according to the conditions required by the application purpose. A wide variety of applications can be achieved by changing the antenna geometry, substrate material type, and feed type to achieve the desired performance for the intended use. The basic configuration of a antenna is thin metallic, as shown in Fig 1. [6, 7, 8].

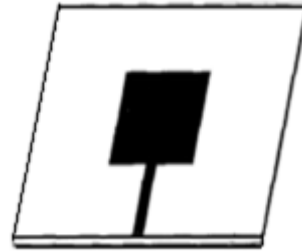


**Fig 1.** Feeding a microstrip rectangular microstrip antenna

The parameters that directly affect the radiation performance of the microstrip antenna are the dimensions and shape of the radiation element, the thickness of the base material and the dielectric constant. Dielectric base material can be selected arbitrarily in accordance with the designed circuit. The dielectric constant and loss tangent of dielectric materials determine the quality of that material. As the value of the loss tangent increases, the antenna efficiency decreases. In microstrip antennas, one side of the dielectric base material is completely covered with the ground plane, while the other side has a planar conductive strip of any geometry. The structure of this strip determines the properties of the antenna [9].

Microstrip antennas are often preferred due to their low profile, lightweight, low cost, ease of integration with arrays or microwave integrated circuits, and polarization diversity [10]. As shown in Table 1, microstrip antennas have applications in both military and civilian sectors.

**Table 1.** Some application areas of microstrip antennas

<b>Platform</b>	<b>Systems</b>
<b>Aircraft</b>	Radar, communications, navigation
<b>Missiles</b>	Telemetry
<b>Satellites</b>	Remote sensing, communication, direct TV broadcasting
<b>Ships</b>	Navigation
<b>Land Vehicles</b>	Mobile satellite phone and mobile radio
<b>Other</b>	Biomedical systems

## 3. MICROSTRIPS PATCH ANTENNAS

In its most basic form, a microstrip patch antenna consists of a ground plane, a dielectric layer and a radiating patch, as shown in Fig 2 [11, 12, 13].

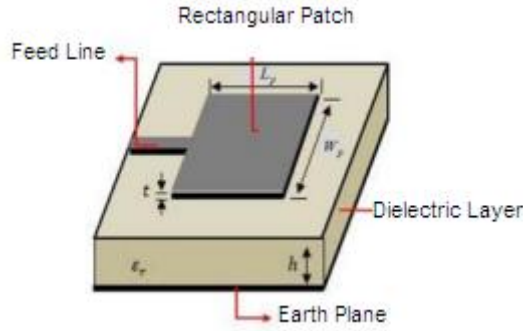


**Fig 2.** Rectangular microstrip patch antenna

The patch on the upper surface is made of conductive materials such as gold or copper. The characteristic feature of this type of antenna is determined by the geometry of the patch on the radiation surface. The geometric shape of the conductor to be used may vary depending on the area to be used or design features. Square, triangle, circle, ellipse etc. They can be used in different ways. Fig 3 shows the geometric shapes of the microstrip patch antenna.

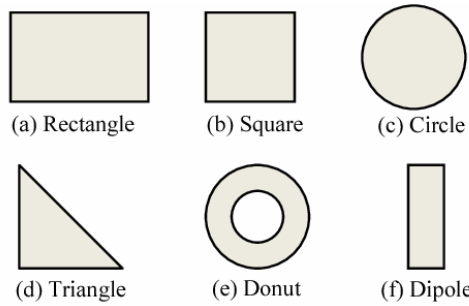


**Fig 3.** Microstrip patch antenna geometric shapes

In microstrip patch antennas, the radiation characteristics remain similar despite variations in the geometric shape of the conducting patch. Their gains are generally around 5–6 dBi and they have a beam width of 3 dB between 70° and 90° [14].

#### 4. TRANSMISSION LINE MODEL FOR RECTANGULAR MICROSTRIP PATCH ANTENNA

The most common patch geometry in terms of usage area is rectangular shaped patches. The width of the radiating patch is shown in Fig 2, where  $W_p$  is its length,  $L_p$  is the dielectric constant of the substrate (dielectric layer) used  $\epsilon_r$  and its thickness is  $h$ . In the mathematical model, first the microstrip patch width  $W_p$  and length  $L_p$  values are found depending on the operating frequency of the antenna and the determined dielectric constant [15]. Width of rectangular patch  $W_p$

$$W_p = \frac{1}{2f_r \sqrt{\mu_0 \epsilon_0}} \sqrt{\frac{2}{\epsilon_r + 1}} = \frac{c}{2f_r} \sqrt{\frac{2}{\epsilon_r + 1}} \tag{1}$$

It can be calculated with the equation. Here  $c$  is the speed of light,  $f_r$  is the resonance frequency, dielectric constant of the gap,  $\epsilon_0$  is the magnetic permeability of the gap.

Since there is a patch on the upper surface of the microstrip antenna and a dielectric layer and air on the lower surface, it has a non-homogeneous structure. This structure causes the electrical permeability value to change. The effective dielectric constant  $\epsilon_{reff}$  for the new case is calculated by equation (2).



$$\frac{W_p}{h} > 1 \tag{2}$$

$$\epsilon_{eff} = \frac{\epsilon_r + 1}{2} + \frac{\epsilon_r - 1}{2} \left[ 1 + 12 \frac{h}{W} \right]^{-1/2} \tag{3}$$

The electric field causes the patch to behave as if it is electrically larger than its physical size. The electrical length of the  $L_{eff}$  patch and the fringing area around the  $\Delta L$  patch are calculated by equations (4) and (5) [13].

$$\Delta L = 0.412h \frac{(\epsilon_{eff} + 0.3) \left( \frac{W}{h} + 0.264 \right)}{(\epsilon_{eff} - 0.258) \left( \frac{W}{h} + 0.8 \right)} \tag{4}$$

$$L_{eff} = \frac{1}{2f_r \sqrt{\epsilon_{eff}} \sqrt{\mu_o \epsilon_o}} \tag{5}$$

If the actual length of the patch is  $L_p$ , it is calculated by equation (6).

$$L_p = L_{eff} - 2\Delta L = \frac{1}{2f_r \sqrt{\epsilon_{eff}} \sqrt{\mu_o \epsilon_o}} - 2\Delta L \tag{6}$$

The dimensions of the dielectric material are given in equation (7) and equation (8).

$$W_m = 6h + W \tag{7}$$

$$L_m = 6h + L \tag{8}$$

Length of indentation,  $y_0$

$$R_{in}(y = y_0) = \frac{1}{2(G_1 \pm G_{12})} \cos^2 \left( \frac{\pi}{L} y_0 \right) \tag{9}$$

$$= R_{in}(y = 0) \cos^2 \left( \frac{\pi}{L} y_0 \right) = \frac{1}{2G_1} \cos^2 \left( \frac{\pi}{L} y_0 \right)$$

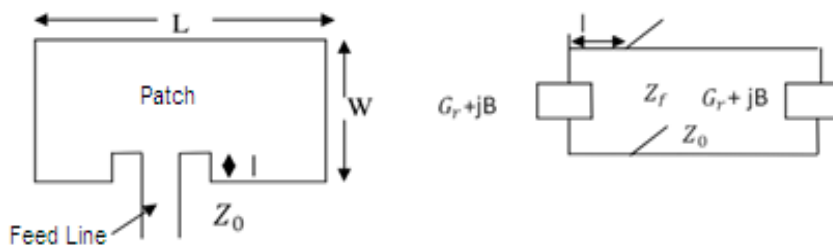


Fig 4. Modeling of microstrip patch antenna

## 5. ANTENNA DESIGN AND SIMULATION

Antennas are created by placing a radiating plane onto the dielectric substrate in the desired geometry. Thickness, type and dielectric constant of the base material; It is important in design because it directly affects the antenna's characteristics such as bandwidth and radiation. Therefore, the first thing to do for microstrip antenna design is to choose a suitable base material. The patch and ground plane generally have regular geometries. Although the patch geometry that provides radiation is generally planar, non-planar geometries are also used [16].

In the study, FR-4 material with a relative dielectric constant ( $\epsilon = 4.3$ ), loss tangent of  $\tan \delta = 0.019$  was preferred as the suitable substrate material, and the dielectric material thickness was preferred as  $h = 1.6$  mm. The designed microstrip antenna is desired to operate at 2.4 GHz operating frequency and the software called CST Microwave Studio was used for the design. The geometry of the microstrip patch antenna to be designed is given in Fig 5. Here, the width of the patch is denoted by  $W$ , the length of the patch is denoted by  $L$ , and the dimensions of the dielectric material are denoted by  $W_m$  and  $L_m$

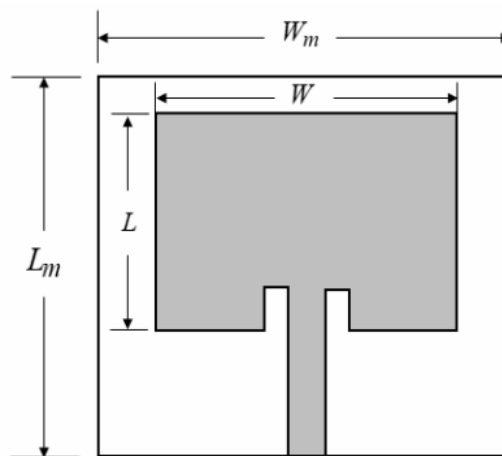


Fig 5. Rectangular microstrip patch antenna geometry

Table 2. Dimensions of the designed patch antenna

Patch Width ( $W$ )	38.39 mm
Patch Length ( $L$ )	28.77 mm
Material Width ( $W_m$ )	100 mm
Material Length ( $L_m$ )	100 mm
Feed Line Width ( $W_p$ )	3.13 mm
Indent Width ( $y_m$ )	1.5 mm
Indent Length ( $y_0$ )	7.0 mm
Grounding Thickness	0.035 mm

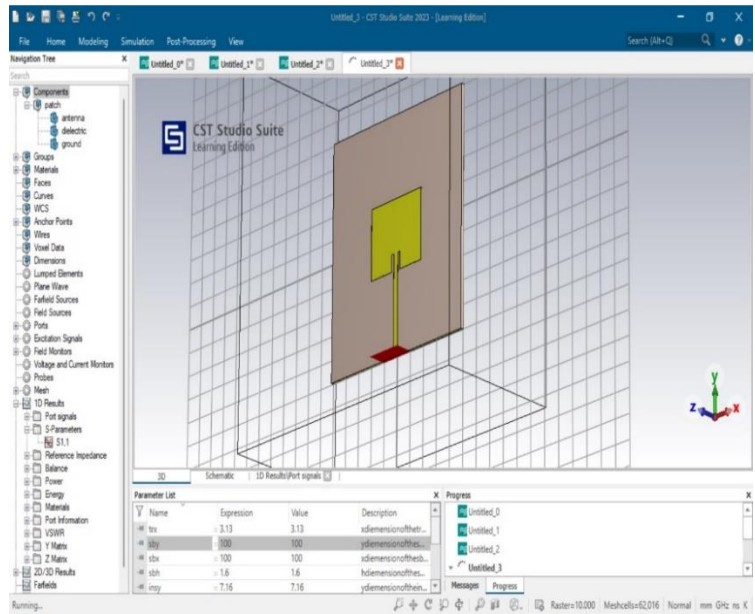


Fig 6. CST Studio representation

## 6. RESULTS

The reflection coefficient of the designed rectangular microstrip patch antenna is given in Fig 7.

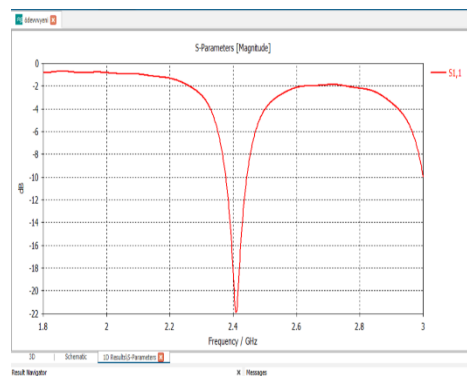


Fig 7. S<sub>11</sub> graph

The gain and directivity diagrams of the antenna are given in Fig 8 and Fig 9. Antenna at 2.4 GHz resonance frequency; It has a maximum gain of 2.27 dB and a maximum directivity of 7.28 dB in the same direction.

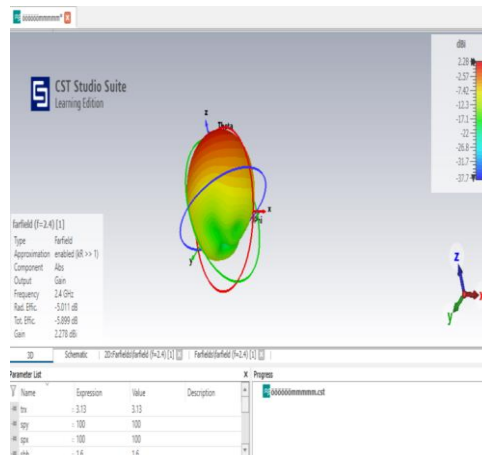


Fig 8. Gain diagram

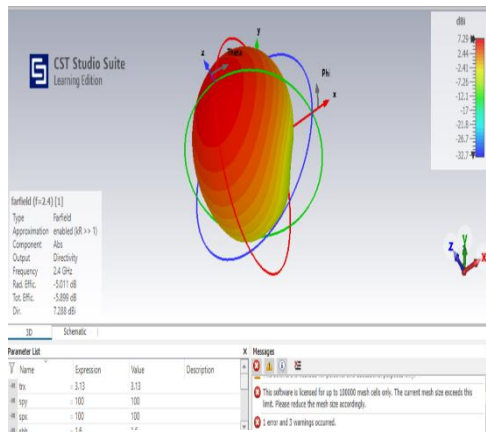


Fig 9. Directivity diagram

The power gain radiation diagram is shown in Fig 10. The radiation diagram is a graph that shows the angular change of the power (electromagnetic field intensity) emitted by the antenna in a certain distant area of the antenna, at a fixed distance. It was determined that Phi 270 value had a maximum directivity of 7.28 dB and a maximum gain of 2.27 dB in the same direction.

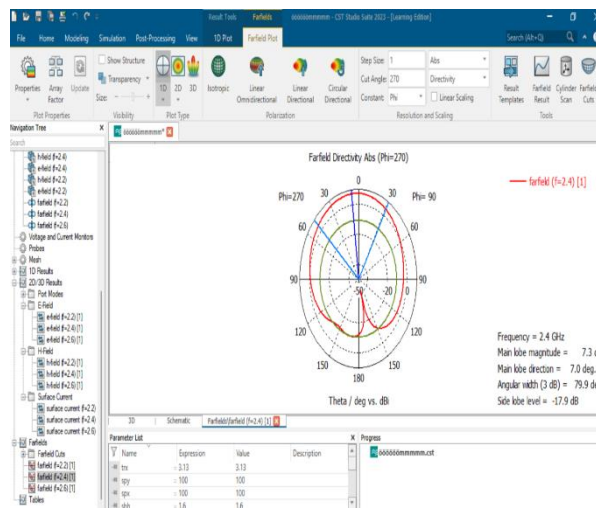


Fig 10. Power gain radiation diagram

Table 3. Comparison of the designed study with the previous study

References	Operating Frequency (in GHz)	Gain (dB)	Max. Directivity (dB)	Return Loss (dB)
[16]	2.4	2.97	3.3	-16
Proposed Antenna	2.4	2.27	7.28	-22

## 7. CONCLUSIONS

Microstrip antennas; They are highly preferred in communication systems because they can be produced cheaply with modern printed circuit technology, have small dimensions, do not damage the structures to be joined, and do not consume too much power. Within the scope of this study; In the 2.4 GHz band, which is widely used in wireless communication systems, a microstrip line with a characteristic impedance of 50 Ω was used. With developing technology; An antenna design has been made to meet the need for broadband microstrip patch antenna designs arising from reasons such as increasing the data transfer rate and uninterrupted data transfer. According to the simulation results made with the CST Microwave Studio program, the antenna at the 2.4 GHz resonance frequency; It was determined that Phi 270 value had a maximum directivity of 7.28 dB and a maximum gain of 2.27 dB in the same

direction. Aiming to achieve the desired performance for the intended use in future studies; A wide variety of applications can be achieved by changing the antenna geometry, substrate material type, and feed type.

## ORCID

Ozlem COSKUN  <https://orcid.org/0000-0001-8800-4433>

Nazlihan ERGINYUREK  <https://orcid.org/0009-0003-3180-3922>

## REFERENCES

- [1]. Gungoren, B., Tekbasi, M., Kayabasi, A. (2019). Rectangular microstrip antenna designs and implementation with different sizes and feeding methods working at 2.4 GHz frequency. *KMU Journal of Engineering and Natural Sciences*, Volume 1, Issue 1, 50-58.
- [2]. R, Azim et al., (2021). A multi-slotted antenna for LTE/5G Sub-6 GHz wireless communication applications. *International Journal of Microwave and Wireless Technologies*, vol. 13, no. 5, pp. 486–496.
- [3]. Karthick, M. (2015). Design of 2.4GHz patch antenna for WLAN applications. 2015 IEEE 7th National Conference on Computing, Communication and Information Systems, NCCIS 2015, pp. 1–4.
- [4]. Tansarikaya, I. (2007). Broadband patch antenna design (Master's Thesis). Istanbul Technical University Institute of Science and Technology.
- [5]. Basaran, C. (2008). Slit ring microstrip antenna design for wireless communication (Doctoral Thesis), Kocaeli University University of Science and Technology.
- [6]. Lai, H. W., Luk, K. M., Leung, K. W. (2013). Dense dielectric patch antenna—A new kind of low-profile antenna element for wireless communications. *IEEE Transactions on Antennas and Propagation*, 61 (8): 4239-4245.
- [7]. Ozturk, A. (2020). Adjustable microstrip balun filter design for new generation communication systems (Master's Thesis). Pamukkale University Institute of Science and Technology.
- [8]. Ibrahimli, I. (2017). Microstrip antenna design in mobile communication (Master's Thesis). Istanbul Aydin University Institute of Science and Technology.
- [9]. Emin, B. (2019). Directional antenna design for long distance communication (Master's Thesis). Nevşehir Hacı Bektaş Veli University Institute of Science and Technology.
- [10]. Uzer, D. (2016). Investigation of Suitable methods for broadband micro strip patch antenna designs (Doctoral Thesis). Selçuk University Institute of Science and Technology.
- [11]. Balanis, C. A. (1982). *Antenna theory analysis and design*. John Wiley and Sons, Arizona State University pages: 4-6
- [12]. Zoukalne, K., Chaib, o A. ve Khayal, M. Y. (2020). Design of microstrip patch antenna array for 5G resonate at 3.6 GHz. *Current Journal of Applied Science and Technology*, 39, no. 34, pp. 164-170.
- [13]. Prajapati, P. R., Murthy, G. G. K., Patnaik, A., Kartikeyan, M. V. (2015). Design and testing of a compact circularly polarized microstrip antenna with fractal defected ground structure for L-band applications. *IET Microwaves, Antennas and Propagation*, vol.9, no. 11, pp. 1179-1185.
- [14]. Li, L. W., Li, Y. N., Yeo, T. S., Mosig, J. R., Martin, O. J. (2010). A broadband and high-gain metamaterial microstrip antenna. *Applied Physics Letters*, 96 (16): 164101.
- [15]. Pozar, D. M. (2012). *Microwave engineering*, Fourth edition, Wiley.
- [16]. Keskin, S. E., Guler, C., Aymaz, R. B., Gursoy, G. S., Ozbey, (2019). 2.4 GHz wideband microstrip antenna design. *Kirklareli University Journal of Engineering and Science* 5-1, pp.1-14.

# Development of an Artificial Intelligence Based Correction System for Spelling Errors in Product Reviews

Okan ÇİFTÇİ<sup>1</sup>, Sumru NAYİR<sup>1</sup>, Emre Tolga AYAN<sup>1</sup>, Ceren ULUS<sup>2</sup>, M. Fatih AKAY<sup>2</sup>

<sup>1</sup>Department of NLP, Trendyol

<sup>2</sup>Department of Computer Engineering, Çukurova University

## ABSTRACT

E-commerce has experienced rapid growth in recent years and continues to expand dynamically. In this sector, maximizing customer satisfaction and enhancing the shopping experience are recognized as important strategic initiatives. To maximize customer satisfaction, it is essential to accurately determine customer needs and provide appropriate solutions to meet demand. In this context, feedback obtained from customers holds significant importance. However, customer comments often contain spelling errors, complicating the analysis of these comments. This study aims to automatically correct spelling errors in user comments regarding products sold on the e-commerce site Trendyol.com. For this purpose, a system based on transformer architecture has been created. Various spelling error detection and correction models were subsequently developed based on this architecture. Prediction models have been developed using two separate datasets consisting of Trendyol user comments and two additional datasets, including the Turkish Spelling Check Dataset taken from the Hunspell library, and the effects of these four datasets on prediction performance have been examined. The success of the models has been evaluated using the Accuracy metric. The performance of the developed models was also compared with that of the model in the Zemberek library. As a result of the study, it has been observed that the utilization of the Turkish Spelling Check Dataset positively influences prediction performance. The developed system enhanced customer experience by correcting spelling errors in comments.

**Keywords:** Spelling error system, Product reviews, Transformer architecture, Turkish spelling check dataset, Zemberek

## 1. INTRODUCTION

The e-commerce sector has shown significant growth in recent years, driven by rapid technological advancements and digitalization [1]. Companies in this sector continuously expand their consumer base by leveraging the broad access provided by digital platforms, thus diversifying competitive dynamics. This rise in the popularity of e-commerce can be attributed to a global shift in consumer behavior toward digital channels, alongside the convenient, fast, and user-friendly shopping experiences offered by online platforms. Consequently, a steady increase is observed in the user base of e-commerce companies, which, in turn, drives significant growth in transaction volumes. This surge in transactions creates a pressing need for companies to manage high volumes efficiently and underscores the necessity for streamlined process management.

E-commerce platforms revolutionize customer interactions with products and services, enabling real-time feedback that significantly influences purchasing decisions. Customer reviews serve as critical feedback, where users share their experiences with products or services, express satisfaction levels, or raise complaints. These comments not only impact the purchasing decisions of potential customers but also provide businesses with valuable insights for improving product or service quality. Customer reviews may touch on aspects such as product features, quality, customer service, or delivery processes, and are essential for assessing brand reliability and customer satisfaction in the realms of digital marketing and e-commerce. Customer feedback and reviews are vital indicators of product reliability and quality, playing a key role in the decision-making processes of prospective buyers. This dynamic empowers consumers to make more informed decisions and enhances their overall shopping experience. However, the prevalence of spelling and grammar errors in reviews poses a significant issue. As long as comments do not contain harmful content like insults,

\*Corresponding Author Email: [f.cerenulus@gmail.com](mailto:f.cerenulus@gmail.com)

Submitted: 04.11.2024 Revision Requested: 06.11.2024 Last Revision Received: 08.11.2024

Accepted: 11.11.2024 Published Online: 03.12.2024



Burdur  
Mehmet Akif Ersoy  
University Press



Cite this article as: Çiftçi, O., Nayir, S., Ayan, E.T., Ulus, C., Akay, M.F. (2024). Development of an Artificial Intelligence Based Correction System for Spelling Errors in Product Reviews. Scientific Journal of Mehmet Akif Ersoy University, 7(2): 99-108.

DOI: <https://doi.org/10.70030/simakeu.1577809>

<https://dergipark.org.tr/simakeu>



Content of this journal is licensed under a Creative Commons Attribution-NonCommercial 4.0 International License.

profanity, or spam, they are visible to all users. Such errors can negatively affect other customers' perceptions and damage brand reputation. Correcting these errors is essential to prevent confusion, improve readability, and ensure that the intended message is clearly understood. Proper spelling enhances communication quality, lends a professional appearance to the text, and is therefore of great importance. [2]

Automating spelling and grammar error correction is a strategic necessity for e-commerce platforms. By facilitating decision-making based on clear, well-expressed information, platforms contribute to more favorable outcomes. Moreover, enabling users to articulate their thoughts clearly and concisely improves information flow, enhances customer satisfaction, boosts sales, and fosters brand loyalty.

This study aims to automatically correct spelling errors in user comments regarding products sold on the e-commerce site Trendyol.com. For this purpose, various spelling error detection and correction models have been developed, and a system based on transformer architecture has been created.

This study is organized as follows: Section 2 includes relevant literature. Dataset is given in Section 3. Section 5 presents methodology. Details of the system is presented in Section 5. Section 6 presents the results of the study. Section 7 concludes the paper.

## 2. LITERATURE REVIEW

[3] presented a two-step, deep learning-based model for detecting misspelled words in Turkish. This model incorporates character-based, syllable-based, and Byte Pair Encoding (BPE) approaches alongside Long Short-Term Memory (LSTM) and Bi-Directional LSTM (Bi-LSTM) networks. Additionally, a false positive reduction model was integrated to minimize false positives caused by the use of foreign words and abbreviations frequently found on online platforms. The results indicated that the proposed Bi-LSTM model with the BPE tokenizer performed effectively. [4] proposed an LSTM-based classification model that utilizes pre-trained language models to correct erroneous query inputs and spelling mistakes. Model pruning techniques, such as No-Teacher Distillation, were employed to address latency issues. The results demonstrated at least a 16% increase in accuracy. [5] aimed to improve the robustness of predictions by modifying traditional autoregressive encoder-decoder models to address spelling correction challenges. Various methods were tested, and a comparative analysis was conducted. [6] proposed a solution to enhance spelling error correction in search queries within e-commerce. Various types of spelling errors were systematically analyzed and categorized. A Transformer model was employed along with synthetic data generation techniques for contextual spelling correction, showing significant improvements over multiple models on both human-labeled data and online A/B experiments. [7] introduced a new method for spelling correction in search queries or single words using a procedure for generating artificial spelling errors. This technique was used to train a generative spelling correction model based on a Transformer architecture, outperforming the conventional noise addition approach. [8] proposed a hybrid model using the Bidirectional Encoder Representations from Transformers (BERT) masked language model combined with Levenshtein Distance (LD) for identifying and correcting various spelling errors. Spelling errors were categorized, and a comprehensive dataset was created. The results showed that the system effectively identified and corrected spelling mistakes. [9] developed a modern spell checker model designed for integration into search engines on e-commerce platforms, specifically for Turkish. The results indicated that the typo corrector performed successfully, even beyond search engine contexts. [10] introduced a two-stage framework using pre-trained language models for correcting Thai spelling errors. Character Edit Distance was applied as a post-processing step to improve corrections. Experiments with two standard datasets showed that the model corrected misspelled words with a 60% success rate. [11] proposed two Seq2Seq deep learning-based automatic spelling error detectors and correctors for social media comments, analyzing input words at the phonogram level. The hybrid system demonstrated effective performance. [12] developed a spelling correction system for Indonesian using the LD algorithm, addressing complex language variations and providing more contextually appropriate corrections. The system achieved a Precision rate of 92% and an F1 Score of 90%. [13] presented a multilingual spell checker model tailored to correct user queries for specific product needs. The model was implemented for auto-completion in Adobe product searches and various applications, outperforming general-purpose spell checkers on in-domain datasets. [14] proposed a model that combines spelling correction with query expansion to enhance search engine performance. Document titles were preprocessed, with Term Frequency-

Inverse Document Frequency weighting applied to terms. The LD algorithm corrected typos, and query expansion improved search results. The system was tested on a dataset of 2,045 entries, achieving an average Recall of 95.91%, Precision of 63.82%, and Non-Interpolated Average Precision of 86.29%. [15] used a Masked Language Model and Edit Distance to correct spelling errors, selecting candidates based on Recall (correction rate) metrics. Results showed significant improvement over previous studies. [16] introduced QazSpell, a Kazakh spell-check and auto-correction system. A large web crawl of noisy data was used to understand misspellings, with a substring alignment model applied to detect symmetric and asymmetric patterns in word-error pairs. The model performed well in generating correction suggestions. [17] introduced a new algorithm to improve spelling error detection in Indonesian. The algorithm has been begun by gathering and combining correct and incorrect sentences, employing Bi-LSTM networks and Multi-Head Attention mechanisms to capture sequence complexity. The model achieved an Accuracy rate of 92%. [18] described the development of a model for detecting misspelled Assamese words in digital content. This model considered the context of the expression when determining word spelling. It highlighted that certain Assamese words may have multiple meanings, and even if spelled correctly according to the dictionary, they may be unsuitable for the intended context of a particular expression. Two machine learning techniques, LSTM and BiLSTM, were employed, with the BiLSTM model achieving the highest accuracy rate of 89.52%. The results indicated that the proposed approach significantly enhanced spelling error detection, outperforming previous research on the Assamese language. [19] presented a spelling checker model for detecting misspelled Urdu words. The model utilized dictionary search and edit distance techniques to generate correct spelling suggestions. A hybrid approach incorporating ranking methods such as Soundex, Shapex, LCS, and N-gram was developed to identify the best candidate word. The system demonstrated high accuracy, achieving an F1 score of 94.02%. [20] proposed a model combining a neural network-based language model with an N-gram model to detect and correct specific Vietnamese spelling errors. In experiments, this model achieved an F1 score 1% to 14% higher than other neural network-based language models and was further compared with various N-gram models.

### 3. DATASET

The dataset has been created by analyzing spelling errors in at least 1 million comments on the Trendyol platform. The Turkish Spelling Dataset taken from the Hunspell library [21] has also been incorporated into the main dataset. Table 1 presents the main dataset, while Table 2 shows the dataset with the added Turkish Spelling Check Dataset.

**Table 1.** The main dataset

Dataset Name	Trendyol Reviews
Train Dataset	45000
Test Dataset	2500
Validation Dataset	2500

**Table 2.** The dataset with the added Turkish spelling check dataset

Dataset Name	Trendyol Reviews & Turkish Spelling Check Dataset
Train Dataset	75000
Test Dataset	3000
Validation Dataset	3000

To expand the spelling error dataset, neighboring letters on the Turkish Q keyboard have been identified and replaced with their respective main letters. The sample representation of turkish q keyboard characters and neighbors is given in Figure 1.



```

Self.ascii_char_neighbor_mapping =
    {'q': ['w', 'a', 's'],
     'w': ['q', 'e', 's', 'd'],
     'e': ['w', 'r', 'd', 's', 'f', '3'],
     'r': ['e', 't', 'f', 'd', 'g'],
     't': ['r', 'y', 'g', 'f', 'h'],
     'y': ['t', 'u', 'h', 'g', 'j'],
     'u': ['y', 'i', 'j', 'h', 'k'],
     'i': ['u', 'o', 'k', 'j', 'l'],
     'o': ['i', 'p', 'l', 'k'],
     'p': ['o', 'l', 'i'],
     'a': ['s', 'q', 'z', 'w', 'x'],
     's': ['a', 'd', 'w', 'x', 'e', 'q', 'z', 'c'],
     'd': ['s', 'f', 'e', 'c', 'r', 'w', 'x', 'v'],
     'f': ['d', 'g', 'v', 'r', 't', 'e', 'c', 'b'],
     'g': ['f', 'h', 't', 'b', 'y', 'r', 'v', 'n'],
     'h': ['g', 'j', 'y', 'n', 'u', 't', 'b', 'm'],
     'j': ['h', 'k', 'u', 'm', 'i', 'y', 'n'],
     'k': ['j', 'l', 'i', 'o', 'u', 'm'],
     'l': ['k', 'o', 'p', 'i'],
     'z': ['x', 'a', 's'],
     'x': ['z', 'c', 's', 'd', 'a'],
     'c': ['x', 'v', 'd', 'f', 's'],
     'v': ['c', 'b', 'f', 'g', 'd'],
     'b': ['v', 'n', 'g', 'h', 'f'],
     'n': ['b', 'm', 'h', 'j', 'g'],
     'm': ['n', 'j', 'k', 'h'],
     ' ': ['c', 'v', 'b', 'n', 'm']}
    
```

**Fig 1.** The sample representation of Turkish q keyboard characters and neighbors.

During dataset preparation, various error types, including omission, insertion, combination, substitution, transposition, splitting, and identity errors, have been considered. The types of errors considered are described below.

1. Omission: A letter is randomly removed from the word.
2. Addition: A letter is randomly added to the word.
3. Combination: A new word is created by combining two existing words.
4. Substitution: A randomly selected letter is replaced with one of its neighboring letters.
5. Transposition: The positions of two letters within the word are swapped.
6. Division: The word is randomly split into two parts.
7. Identity: The word is left unchanged.

As a result of the operations performed, four different datasets have become ready. The high-quality and diverse spelling error dataset is presented in Table 3.

**Table 3.** The high quality and diverse spelling error dataset

Error Text	Dataset	Error Distribution	Dataset Size	Output Size
A1	trendyol_reviews.csv	"identity": 0.10, "insertion": 0.16, "omission": 0.16, "substitution": 0.08, "transposition": 0.16, "combination": 0.16, "split": 0.13, "english": 0.02, "shuffle": 0.0, "minedit": 0.03, "phonetic": 0.0	45000	135000
A2	trendyol_reviews.csv	"identity": 0.10, "insertion": 0.10, "omission": 0.10, "substitution": 0.14, "transposition": 0.19, "combination": 0.19, "split": 0.13, "english": 0.02, "shuffle": 0.0, "minedit": 0.03, "phonetic": 0.0	45000	135000
A3	trendyol_reviews_data_and_h_unspell.csv	"identity": 0.10, "insertion": 0.16, "omission": 0.16, "substitution": 0.08, "transposition": 0.16, "combination": 0.16, "split": 0.13, "english": 0.02, "shuffle": 0.0, "minedit": 0.03, "phonetic": 0.0	75000	300000
A4	trendyol_reviews_data_and_h_unspell.csv	"identity": 0.10, "insertion": 0.10, "omission": 0.10, "substitution": 0.14, "transposition": 0.19, "combination": 0.19, "split": 0.13, "english": 0.02, "shuffle": 0.0, "minedit": 0.03, "phonetic": 0.0	75000	300000

## 4. METHODOLOGY

### 4.1 Transformers Architecture

Before the development of transformers, machine translation and sequential data processing tasks commonly used encoder-decoder architectures, typically employing Recurrent Neural Network (RNN), LSTM, or Gated Recurrent Unit cells. In these architectures, often referred to as Seq2Seq models, input tokens are encoded into hidden states through multiple RNN cells. These encoded hidden states are then combined before being passed to the decoder. Decoders can leverage all encoded data to predict output tokens using these hidden states. However, although the last hidden state from the encoder contains substantial meaning and context, this information may not be fully captured by the Seq2Seq decoder. This issue, known as the 'bottleneck problem,' implies that as the input sequence grows longer and more complex, the hidden state becomes less effective. The attention mechanism addresses this limitation by allowing simultaneous processing of multiple inputs. During this process, it generates weight matrices for each hidden state and computes a weighted sum of all previous encoder states, enabling the decoder to identify which hidden states to "pay more attention" to. Since Seq2Seq architecture processes input sequentially, the information from the previous hidden state (t-1) is required to calculate the token at the current time (t). This sequential processing may hinder the correction of final tokens, particularly in tasks with numerous erroneous tokens, such as spelling correction. The limitations of these earlier systems are overcome by the transformer architecture and its attention mechanism. The transformer, based on the encoder-decoder structure, incorporates fully connected layers and multi-head self-attention mechanisms. This structure minimizes performance degradation from long dependencies and enables parallel computation. Positional embeddings and multi-head self-attention encode additional information about token positions and inter-token relationships [22].

### 4.2 Zemberek Library

Zemberek's current goal is to offer a general (Natural Language Processing – NLP) framework for other, largely ignored Turkic Languages in addition to Turkish. At the moment, the framework offers fundamental NLP functions like spell checking, morphological parsing, stemming, word construction, word suggestion, word conversion from words written exclusively in American Standard Code for Information Interchange characters (also known as "deasciifier"), and syllable extraction. To facilitate the work of language developers, Zemberek externalizes some language data to text-based configuration files. However, externalization typically has a negative impact on performance and flexibility. As a result, certain details are retained in the code, such as special cases and the suffix production mechanism [23].

## 5. DETAILS OF THE SYSTEM

The Seq2Seq architecture based on the encoder-decoder structure has been designed for training the obtained dataset. The variations of the created dataset have been diversified using different options. The constructed architecture has been trained in various configurations with different hyperparameters. Figure 2 illustrates the transformer architecture.

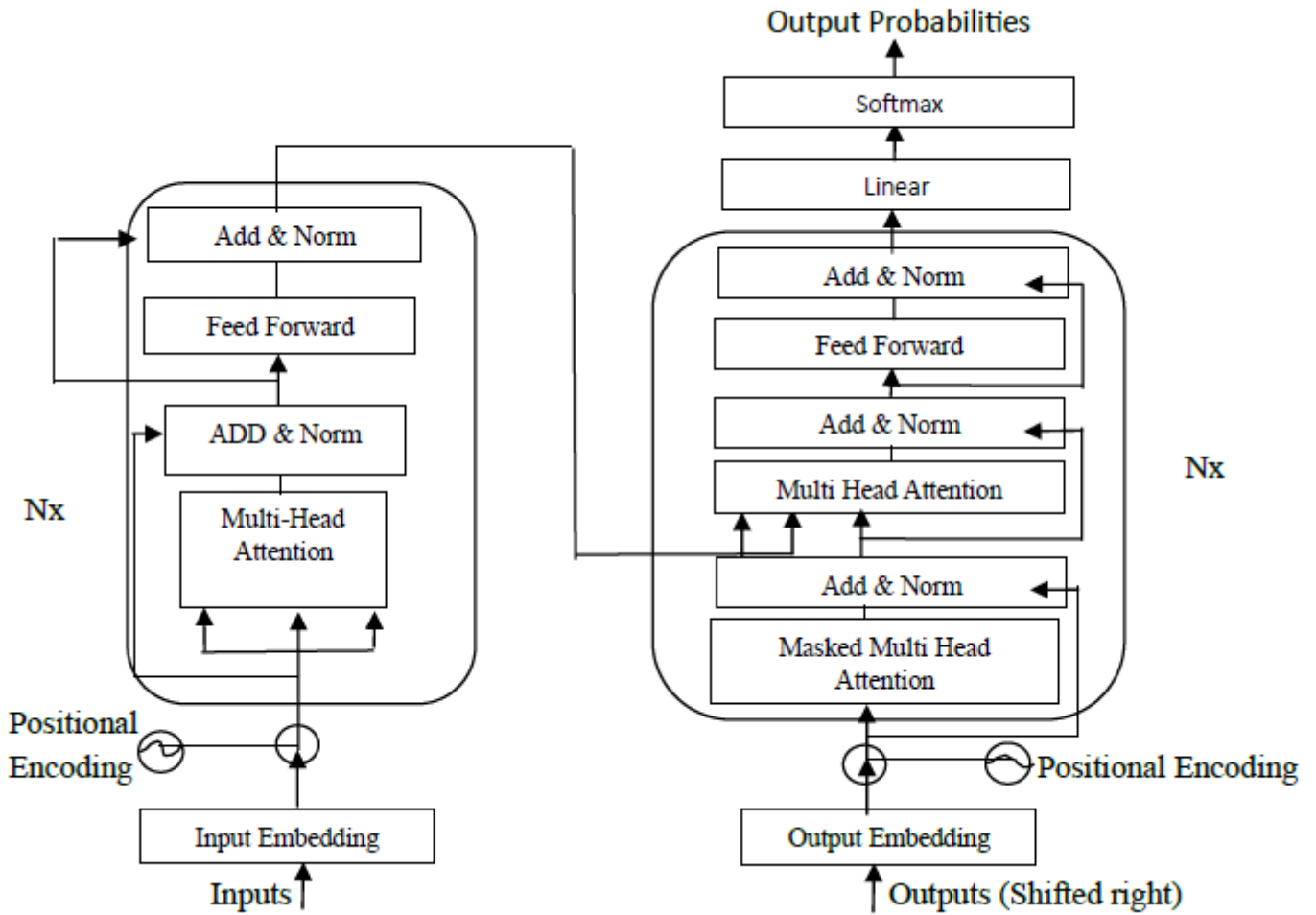


Fig 2. Transformer architecture

Models for spelling error detection and correction have been developed. Models A1, A2, A3, and A4 have been developed for four distinct datasets. The parameters such as hidden dimension, encoder/decoder layers, number of epochs and number of errors have been evaluated in different combinations. In addition, the influence of these parameter values on model performance has been systematically examined. In this context, eight different models have been developed. The parameter values of the developed models are presented in Table 4.

Table 4. The parameter values of the developed models

Model Name	Dataset	Hid Dim.	Enc/Dec. Layers	Epoch	Num of Errors
A1-1	A1	128	4/2	8	2
A1-2	A1	256	6/4	10	2
A2-1	A2	128	4/2	8	2
A2-2	A2	256	6/4	10	2
A3-1	A3	128	4/2	8	2
A3-2	A3	256	6/4	10	2
A4-1	A4	128	4/2	8	2
A4-2	A4	256	6/4	10	2

Additionally, the performance of the model in the Zemberek library has been tested as an alternative spelling corrector for the developed solution. The validation dataset has been provided as input to this module, and the results obtained have been compared.

## 6. RESULTS AND DISCUSSION

The prediction performance of the developed models has been evaluated with the Accuracy metric. Accuracy has been chosen because the problem at hand is a classification problem. It is widely recognized in the literature as a frequently used and reliable metric for such problems. The Accuracy values of the models obtained using different datasets are presented in Table 5.

**Table 5.** The Accuracy values of the models

Method/Achievement (Accuracy)	Trendyol Reviews-1	Trendyol Reviews-2	Trendyol Reviews & Turkish Spelling Check Dataset-1	Trendyol Reviews & Turkish Spelling Check Dataset-2
A1-1	%78.40	%75.15	%69.50	%68.37
A1-2	%75.75	%71.45	%69.17	%68.98
A2-1	%77.40	%79.10	%70.16	%67.17
A2-2	%73.21	%75.15	%69.35	%70.15
A3-1	%79.45	%79.63	%85.72	%84.37
A3-2	%77.16	%77.72	%80.64	%84.02
A4-1	%79.08	%78.98	%83.27	%81.29
A4-2	%77.02	%76.17	%82.27	%82.79
Model in the Zemberek	%54.48	%55.31	%61.27	%61.74

- Models within the A3 series consistently achieved higher Accuracy rates relative to their counterparts.
- The A3-1 model stood out as the most successful model by providing 85.72% Accuracy with the Trendyol Reviews & Turkish Spelling Check Dataset-1 and 84.37% Accuracy with the Trendyol Reviews & Turkish Spelling Check Dataset-2. The closest performance to this model has been shown by A3-2 with 84.02% Accuracy in the Trendyol Reviews & Turkish Spelling Check Dataset-2.
- The A1-1 and A1-2 models lag behind the leading A3 models, recording Accuracy rates of 78.40% and 75.75%, respectively.
- The Accuracy rates obtained through the model in the Zemberek library, specifically 54.48%, 55.31%, 61.27%, and 61.74%, are markedly lower than those of the other models. This finding suggested that the model in the Zemberek library is less effective for the datasets under consideration.
- The prediction models developed using the Trendyol reviews datasets exhibited similar performance.
- The models developed with the Trendyol Reviews & Turkish Spelling Check Datasets delivered more accurate forecast results than those developed with the Trendyol reviews datasets.
- It has been observed that the forecast models developed with the Trendyol Reviews & Turkish Spelling Check Dataset-1 and Trendyol Reviews & Turkish Spelling Check Dataset-2 datasets showed similar performance.

Overall, the A3 series models, particularly A3-1 and A3-2, achieved the highest performance. Incorporating the Trendyol Reviews & Turkish Spelling Check Dataset appears to enhance overall accuracy rates, while the Zemberek library model demonstrates lower performance across all models, failing to produce sufficient results for these datasets. When the results obtained with the developed prediction models have been examined, it has been observed that the transformer-based architecture exhibits satisfactory performance in detecting and correcting spelling errors.

An example of a comment processed by the developed system is provided below. The first sentence displays the raw comment received as input from the user. The second sentence shows the corrected version of this comment, with spelling errors addressed by the system.

“2 tne aldım denemek için çok güzeldi 3 tne daha sipariş verdim stoklamak için teşekkürler.”

“2 tane aldım denemek için çok güzeldi 3 tane daha sipariş verdim stoklamak için teşekkürler.”

Sample outputs have been obtained using FastAPI Swagger. The screenshot of the outputs is shown in Figure 3.

text string (query)	ayakkab rengi resimlerle uyumlu <small>maxLength: 100</small>
x- agentname string (header)	t
x- correlationId string (header)	t


**Fig 3.** FastAPI swagger example outputs


The developed system contributed to improving the customer experience by correcting typos in comments. These findings offer a significant foundation for evaluating the efficacy of the proposed methodologies and highlight opportunities for further refinement and optimization in future research endeavors.


## 7. CONCLUSION


E-commerce has experienced rapid growth in recent years and continues to expand dynamically. To maximize customer satisfaction in this sector, accurately identifying customer needs and developing strategies to meet demand are essential. Customer reviews are valuable for e-commerce platforms; however, they frequently contain typographical errors. In this study, a system has been developed to automatically correct typos in user comments on products sold on the e-commerce site Trendyol.com and models for spelling error detection and correction have been developed. Model performance has been evaluated using the Accuracy metric, revealing that the A3 series models demonstrated the highest performance. This study presents a more up-to-date system compared to previous research. The effect of using Turkish Spelling Check Dataset has been analyzed. In addition, the performance of the developed models has been also compared with the performance of the model in the Zemberek library. The study emphasizes the importance of spelling error detection and provides valuable insights for e-commerce businesses.


## ORCID

Okan ÇİFTÇİ  <https://orcid.org/0000-0002-9435-8980>

Sumru NAYİR  <https://orcid.org/0009-0003-4782-3063>

Emre Tolga AYAN  <https://orcid.org/0000-0002-4894-2190>

Ceren ULUS  <https://orcid.org/0000-0003-2086-6381>

M. Fatih AKAY  <https://orcid.org/0000-0003-0780-0679>

## REFERENCES

- [1]. Sanbella, L., Van Versie, I., & Audiah, S. (2024). Online Marketing Strategy Optimization to Increase Sales and E-Commerce Development: An Integrated Approach in the Digital Age. *Startuppreneur Business Digital (SABDA Journal)*, 3(1), 54-66.
- [2]. Wang, Z., Zhu, Y., He, S., Yan, H., & Zhu, Z. (2024). LLM for sentiment analysis in e-commerce: A deep dive into customer feedback. *Applied Science and Engineering Journal for Advanced Research*, 3(4), 8-13.
- [3]. Aytan, B., & Şakar, C. O. (2023). Deep learning-based Turkish spelling error detection with a multi-class false positive reduction model. *Turkish Journal of Electrical Engineering and Computer Sciences*, 31(3), 581-595.
- [4]. Dutta, A., Polushin, G., Zhang, X., & Stein, D. (2024). Enhancing E-commerce Spelling Correction with Fine-Tuned Transformer Models. In *Proceedings of the 30th ACM SIGKDD Conference on Knowledge Discovery and Data Mining* (pp. 4928-4938). <https://doi.org/10.1145/3637528.3671625>
- [5]. Isbarov, J., Huseynova, K., & Rustamov, S. (2024, April). Robust automated spelling correction with deep ensembles. In *Proceedings of the 2024 8th International Conference on Intelligent Systems, Metaheuristics & Swarm Intelligence* (pp. 26-30). <https://doi.org/10.1145/3665065.3665070>

- [6]. Kakkar, V., Sharma, C., Pande, M., & Kumar, S. (2023, July). Search Query Spell Correction with Weak Supervision in E-commerce. In Proceedings of the 61st Annual Meeting of the Association for Computational Linguistics (Volume 5: Industry Track) (pp. 687-694).
- [7]. Kuznetsov, A., & Urdiales, H. Spelling correction with denoising transformer. arXiv 2021. arXiv preprint arXiv:2105.05977.
- [8]. Naziri, A., & Zeinali, H. (2024). A Comprehensive Approach to Misspelling Correction with BERT and Levenshtein Distance. arXiv preprint arXiv:2407.17383.
- [9]. Oral, E., Mancuhan, K., Erdem, H. V., & Hatipoglu, P. E. (2024, May). Turkish Typo Correction for E-Commerce Search Engines. In Proceedings of the Seventh Workshop on e-Commerce and NLP@ LREC-COLING 2024 (pp. 65-73).
- [10]. Pankam, I., Limkonchotiwat, P., & Chuangsuwanich, E. (2023, June). Two-stage Thai Misspelling Correction based on Pre-trained Language Models. In 2023 20th International Joint Conference on Computer Science and Software Engineering (JCSSE) (pp. 7-12). IEEE.
- [11]. Ratnam, D. J., Karthika, A. N., Praveena, K., Taniya, R., Thara, S., & Prema, N. (2024). Phonogram-based Automatic Typo Correction in Malayalam Social Media Comments. *Procedia Computer Science*, 233, 391-400.
- [12]. Santoso, J. T., & Yan, S. (2024). A Hybrid Approach to Typo Correction in Indonesian Documents Using Levenshtein Distance. *Journal of Technology Informatics and Engineering*, 3(2), 151-168.
- [13]. Sharma, S., Valls-Vargas, J., King, T. H., Guerin, F., & Arora, C. (2023, July). Contextual multilingual spellchecker for user queries. In Proceedings of the 46th International ACM SIGIR Conference on Research and Development in Information Retrieval (pp. 3395-3399).
- [14]. Soyusiawaty, D., & Wolley, D. H. R. (2021). Hybrid spelling correction and query expansion for relevance document searching. *International Journal of Advanced Computer Science and Applications*, 12(8).
- [15]. Tohidian, F., Kashiri, A., & Lotfi, F. (2022, November). BEDSpell: Spelling Error Correction Using BERT-Based Masked Language Model and Edit Distance. In International Conference on Service-Oriented Computing (pp. 3-14). Cham: Springer Nature Switzerland.
- [16]. Toleu, A., Tolegen, G., Mussabayev, R., Krassovitskiy, A., & Ualiyeva, I. (2022). Data-driven approach for spellchecking and autocorrection. *Symmetry*, 14(11), 2261.
- [17]. Yanfi, Y., Soeparno, H., Setiawan, R., & Budiharto, W. (2024). Multi-head Attention Based Bidirectional LSTM for Spelling Error Detection in the Indonesian Language. *IEEE Access*.
- [18]. Phukan, R., Neog, M., & Baruah, N. (2023, July). A Deep Learning Based Approach For Spelling Error Detection In The Assamese Language. In 2023 14th International Conference on Computing Communication and Networking Technologies (ICCCNT) (pp. 1-7). IEEE.
- [19]. Aziz, R., Anwar, M. W., Jamal, M. H., & Bajwa, U. I. (2021). A hybrid model for spelling error detection and correction for Urdu language. *Neural Computing and Applications*, 33, 14707-14721.
- [20]. Tien, D. N., Minh, T. T. T., Vu, L. L., & Minh, T. D. (2022). Vietnamese Spelling Error Detection and Correction Using BERT and N-gram Language Model. In *Intelligent Systems and Networks: Selected Articles from ICISN 2022, Vietnam* (pp. 427-436). Singapore: Springer Nature Singapore.
- [21]. Al-Hussaini, L. (2017). Experience: insights into the benchmarking data of hunspell and aspell spell checkers. *Journal of Data and Information Quality (JDIQ)*, 8(3-4), 1-10.
- [22]. Do, D. T., Nguyen, H. T., Bui, T. N., & Vo, H. D. (2021). Vsec: Transformer-based model for vietnamese spelling correction. In *PRICAI 2021: Trends in Artificial Intelligence: 18th Pacific Rim International Conference on Artificial Intelligence, PRICAI 2021, Hanoi, Vietnam, November 8–12, 2021, Proceedings, Part II 18* (pp. 259-272). Springer International Publishing.
- [23]. Akin, A. A., & Akin, M. D. (2007). Zemberek, an open source NLP framework for Turkic languages. *Structure*, 10, 1-5.

# Using Musical Notes and Artificial Intelligence Together as a Tool in Spatial Design

Hüseyin Samet AŞIKKUTLU<sup>1\*</sup>, Latif Gürkan KAYA<sup>1</sup>, Betül Halime UZUNAY<sup>2</sup>

<sup>1</sup>Department of Landscape Architecture, Burdur Mehmet Akif Ersoy University

<sup>2</sup>Department of Design, Burdur Mehmet Akif Ersoy University

## ABSTRACT

It is possible to state that it is an important issue to follow different methods or current issues in revealing spatial design approaches. Thus, it will be possible to create spaces with unique and remarkable qualities. Music can be a tool that can be used or utilized in spatial design processes. The aim of this study is to explore the outcomes of combining musical notes and artificial intelligence to develop suggestions and alternatives for spatial design. The material of the study consists of national and international literature on the subject, a song sample selected specifically for the subject, AutoCAD, 3ds Max, Corona Renderer programs and PromeAI artificial intelligence program. In this context, three-dimensional visuals were created using computer programs based on the notes and sound waves of the selected song and alternatives based on these visuals were put forward. As a result, it is possible to state that the use of musical notes together with computer and artificial intelligence programs will be effective for designers to reveal faster, remarkable and innovative spatial design approaches.

**Keywords:** Artificial intelligence, Music, Note, Space, Spatial design.

## 1. INTRODUCTION

Music, which has an important place in human life [1], is both a translator of emotions and a powerful structure that can affect every aspect of our lives [2,3]. Therefore, music has interacted with many branches of art and is structurally associated with the concept of time and existentially associated with the concept of space. Music can be used to determine the form in design, and it is possible to create space in line with the data obtained from music. In this context, it can be stated that music can be included in the space and even conceptually evaluated and the space can be organized [4].

In the 6<sup>th</sup> century BC, Ancient Greek philosopher Pythagoras introduced the Theory of the Music of the Spheres, connecting music and arithmetic to achieve perfect harmony, which he described as the ultimate standard of absolute harmony. Pythagoras discovered that musical notes could be spatially interpreted by vibrating two strings of proportional size under the same conditions. If the strings are in a 1:2 ratio (diapason), the shorter string produces a note one octave higher than the longer one. When the strings are related in a ratio of 2:3 (diapente), the difference in height corresponds to one fifth. When the ratio is 3:4 (diatessaron), there is a difference of a quarter. Thus, the harmonies of the Greek musical system are expressed in the sequence 1:2-2:3-3:4, which is composed of the first four integers believed to determine the secret of the ideal harmony that reigns in the universe [5]. Pythagoras is said to have realized that when he heard the rhythmic sounds made by blacksmiths striking the anvil with hammers, he realized that these strikes were in a numerical and geometric order. This leads to the idea that the microcosm and macrocosm of the universe may have the same harmonic principles. According to him, the universe actually shows an ideal order of sounds. The intervals in music express a structural reflection of the universe. The interval of each note is proportional to the absolute orbital distances of the planets, and this works in harmony with the sounds that reach a human ear. According to Pythagoras, nature is manifested in the microcosm and the human body is organized in perfect proportions. These Pythagoras' ideas and traditions are still alive today [6].

\*Corresponding Author Email: [sasikkutlu@mehmetakif.edu.tr](mailto:sasikkutlu@mehmetakif.edu.tr)

Submitted: 30.10.2024 Revision Requested: 21.11.2024 Last Revision Received: 27.11.2024

Accepted: 27.11.2024 Published Online: 05.12.2024

Cite this article as: Aşıkutlu, H.S., Kaya, L.G., Uzunay, B.H. (2024). Using Musical Notes and Artificial Intelligence Together as a Tool in Spatial Design. Scientific Journal of Mehmet Akif Ersoy University, 7(2): 109-116.

DOI: <https://doi.org/10.70030/simakeu.1576148>



Burdur  
Mehmet Akif Ersoy  
University Press



<https://dergipark.org.tr/simakeu>



Content of this journal is licensed under a Creative Commons Attribution-NonCommercial 4.0 International License.



Regarding the use of musical notes in spatial design processes, Egidio Jiménez [7] stated in his study that Chartres Notre Dame Cathedral is in perfect harmony in terms of its dimensions and proportions and that it is shapely representative. He also stated that the building was constructed with a musical proportion hidden in the floor plan and the geometry of the west facade. Figure 1 presents visuals of the facade views and floor plan of Chartres Notre Dame Cathedral.

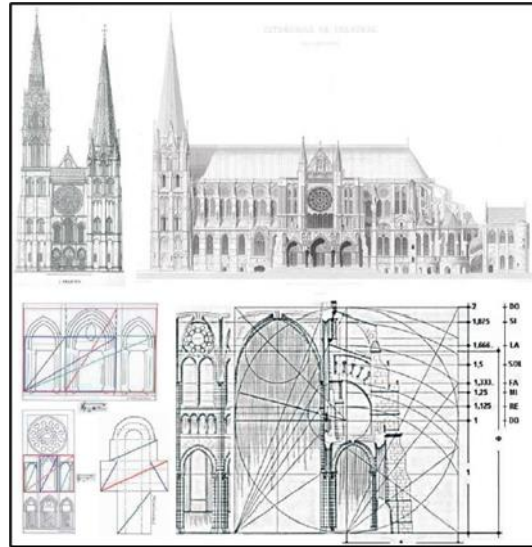


**Fig 1.** Visuals of the facade views and floor plan of Chartres Notre Dame Cathedral [7]

In a different vein, Egidio Jiménez [7] stated in his study that Villa Foscari is an important example of the use of musical proportions and numerical values in space design. He also emphasized that the harmony of spatial proportions and music is seen in the floor plan and facade of the building. In Figure 2, visuals of Villa Foscari's facade views and floor plan are presented.

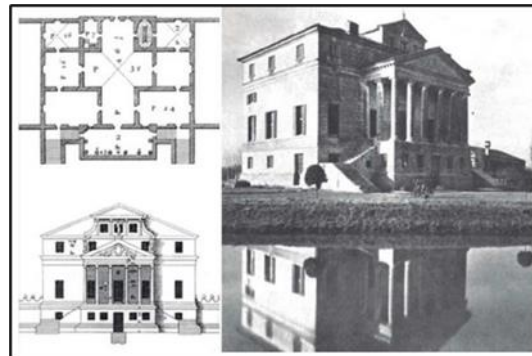


**Fig 2.** Visuals of Villa Foscari's facade views and floor plan [7]

The Stretto House is a building consisting of four sections and is another example of music transformed into a home form based on string and percussion instruments [8]. Figure 3 presents a visual of the design of the Stretto House.

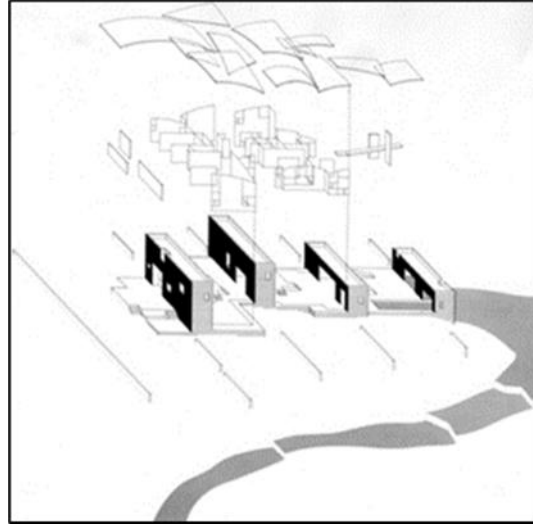


**Fig 3.** Visual of Stretto House's design [8]

Artificial Intelligence (AI) is defined as the intelligence exhibited by an artificial entity to solve complex problems, and such a system is generally assumed to be a computer or machine. AI represents the integration of computer science and physiology. In simple terms, AI is concerned with making computers behave like humans and do so in a much shorter time [9]. In a different assessment, as a branch of science that enables computers to imitate human behavior to help humans to perform better in science and technology, the main goals of AI are to replicate human intelligence, solve knowledge-intensive tasks, build machines that can perform tasks that require human intelligence, and create a self-learning system [10].

In recent years, AI has been increasingly used in the field of spatial design as in many other fields. This means that designers should use AI in the design process [11]. The relationship between AI and space design can be applied in many different fields. By analyzing concepts in the design process, it can constrain or expand design alternatives. However, AI has the potential to automate human-intensive tasks in the design process, which can speed up the design process. It can analyze the data used in space design and use this data to improve the functionality and aesthetics of the space [12]. In short, AI, which is a comprehensive interdisciplinary science field, can produce effective solutions to spatial problems [13]. As a result of the use of AI technologies in space design, the need for manpower decreases and it can be said that the studies are realized with full efficiency [14]. Another way of using AI in space design is to optimize space. By analyzing the data used to optimize the space, AI can offer suggestions that will ensure the best use of the space. For example, AI can increase the functionality of the space by suggesting the most appropriate arrangement according to the intended use of the space [15].

The aim of this study is to create three-dimensional alternatives based on spatial design by using musical notes and AI together and also to put forward suggestions for the use of musical notes in spatial design processes with AI support.

## 2. MATERIALS AND METHODS

The materials for this study include national and international literature on the subject as well as the song 'And She Was' by the Talking Heads. In addition, AutoCAD, 3ds Max, Corona Renderer programs and PromeAI as an AI program constitute the material of the study.

The methodology of the study consists of two stages. In the first stage, it was aimed to develop three-dimensional spatial design visuals. For this purpose, it was inspired by the song "And She Was" by the band "Talking Heads", which Martin Wattenberg used to analyze music in a visual format in his work "The Shape of Song". First of all, the visual situation of the colors and shapes of the song was drawn in two dimensions in AutoCAD program. Different plans were obtained by removing some parts of this design. These plans, created by preserving the proportions in the first figure, were transferred to the 3ds Max program. No function was defined for the forms modeled in the 3ds Max program. Finally, their renderings were taken with the Corona Renderer program used as an add-on to the 3ds Max program. In

the second stage, various functions were defined and visuals were created for these forms through PromeAI as an AI program.

### 3. RESULTS AND DISCUSSION

Martin Wattenberg, a studio musician and data visualization expert, began his 2001 work “The Shape of Song” with the aim of seeing the form of music. In his work, he used a visualization method called arc diagram, which shows the repeated sections of music or any sequence with translucent arc drawings. In this context, Martin Wattenberg analyzed many pieces of music in a visual format, and one of the examples he examined was the song “And She Was” by the band “Talking Heads” (Figure 4) [16].

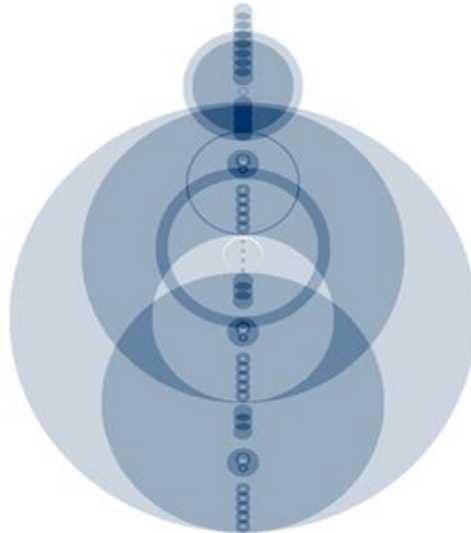


**Fig 4.** Visualized version of “And She Was”, the song of the group “Talking Heads” [16]

In his work, Martin Wattenberg seeks to visually interpret the experience of listening to music. The visual representation of each song presents the melodic and instrumental structures of the song through different colors and forms. This allows listeners to visually explore the song’s structure, rhythm and the interaction of the instruments [17].

The visual of the song “And She Was” of the “Talking Heads” group, which Martin Wattenberg used in his “The Shape of Song” study, drawn in two dimensions in AutoCAD program is presented in Figure 5.

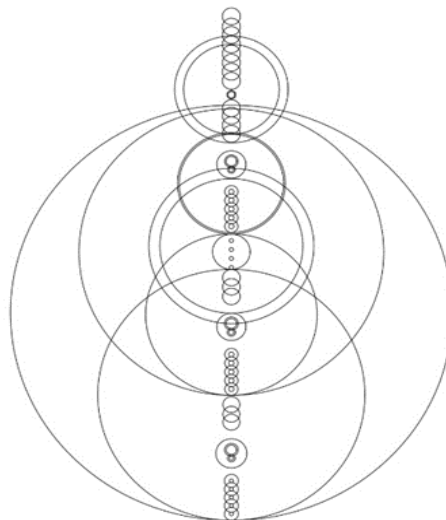


**Fig 5.** Figure of the two-dimensional drawing of the song “And She Was” by the band “Talking Heads” in AutoCAD program

The dense lines and forms in this figure were then simplified before moving on to the form phase. Some lines indicate elevation differences, while others define the ceiling element (Figure 6).

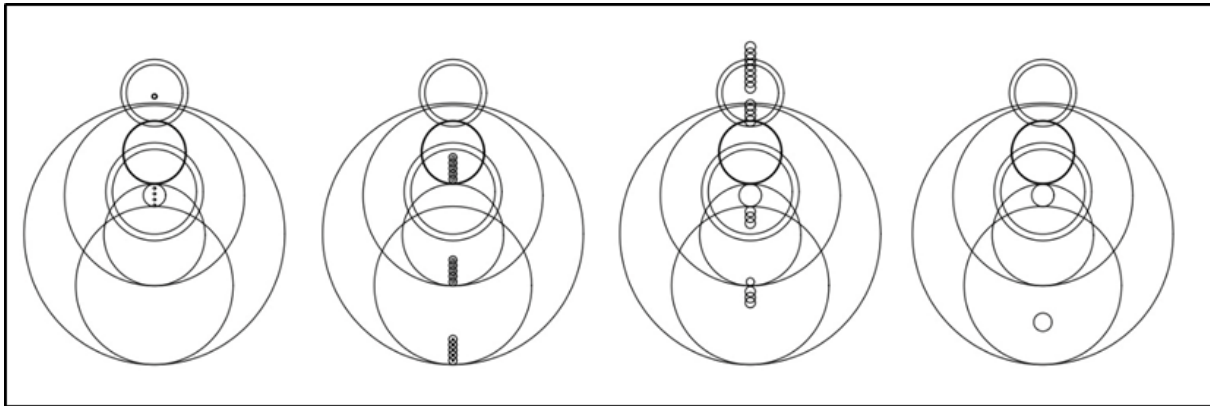


**Fig 6.** Simplified version of the figure transferred to AutoCAD program

Various forms were created using the 3ds Max program and using these lines. The visuals of the forms were rendered with the Corona Renderer program. Finally, various functional approaches to these forms were selected in the AI program PromeAI to make it a more aesthetic and usable space. In Figure 7, the visuals produced for the concretization and interpretation of the abstract structure of the musical notes of the song “And She Was” are presented and the design approaches of these visuals are explained below:

- A stepped roof garden design was created by perceiving the model created in Figure 7a-a1 as a top view. AI evaluated the space created in the middle section as a water element. The model created in Figure 7a-a2 was intended to be an amphitheater design. This amphitheater design, which was placed in the garden of a house with the help of AI, can also be evaluated in a square at a larger scale.
- The model created in Figure 7b expresses an accentuating space created by integrating with the water element. While Figure 7b-a2 is located completely in the center of the water element, in Figure 7b-a1, it is positioned on the edge of the water element and plant elements and an ornamental pool are integrated into it, offering users the opportunity to experience this monument.
- While Figure 7c-a1 can be considered as an accentuating space or square, Figure 7c-a2 has been completely transformed into an architectural structure. The staggered placement of the cylindrical forms has made the architectural structure more effective.
- The model created in Figure 7d-a1 is perceived as a plan and an architectural form or an example of an urban park is revealed. The part seen as wooden veneer can refer to an architectural element, and if this area is considered as a city park, it can also be evaluated as a skateboard track. Figure 7d-a2 perceives the form as three-dimensional and associates it with skyscrapers and evaluates it as a monument in a city with skyscrapers.
- Figure 7e-a1 is interpreted as an area enriched with plant elements within the park area. On the other hand, the form in Figure 7e-a2 is interpreted as a kitchen unit in a completely different context, which shows that the resulting form is versatile and functional.
- In Figure 7f-a1, the form has been transformed into an independent and small space. In this form, an image that can be evaluated as a tiny house, a security hut, a coffee sales unit or a villa entrance unit is provided. Figure 7f-a2 shows the top view of a building unit since it is preferred to evaluate the form as a top view. This view can belong to a restaurant or a detached building.
- Figure 7g was asked to be evaluated in the interior space and different materials and styles were experimented on this form. While a modern image was created with wooden materials in Figure 7g-a1, Figure 7g-a2 was given an industrial appearance with metal materials.
- Figure 7h-a1 expresses a form that can be integrated into children's playgrounds, while Figure 7h-a2 expresses a Moroccan and Marrakech style interior.
- In Figure 7i-a1, an accentuating element is created, while in Figure 7i-a2 the same form is used as an information desk.

	Created Model	Alternative 1 (a1)	Alternative 2 (a2)
Figure 7a			
Figure 7b			
Figure 7c			
Figure 7d			
Figure 7e			
Figure 7f			

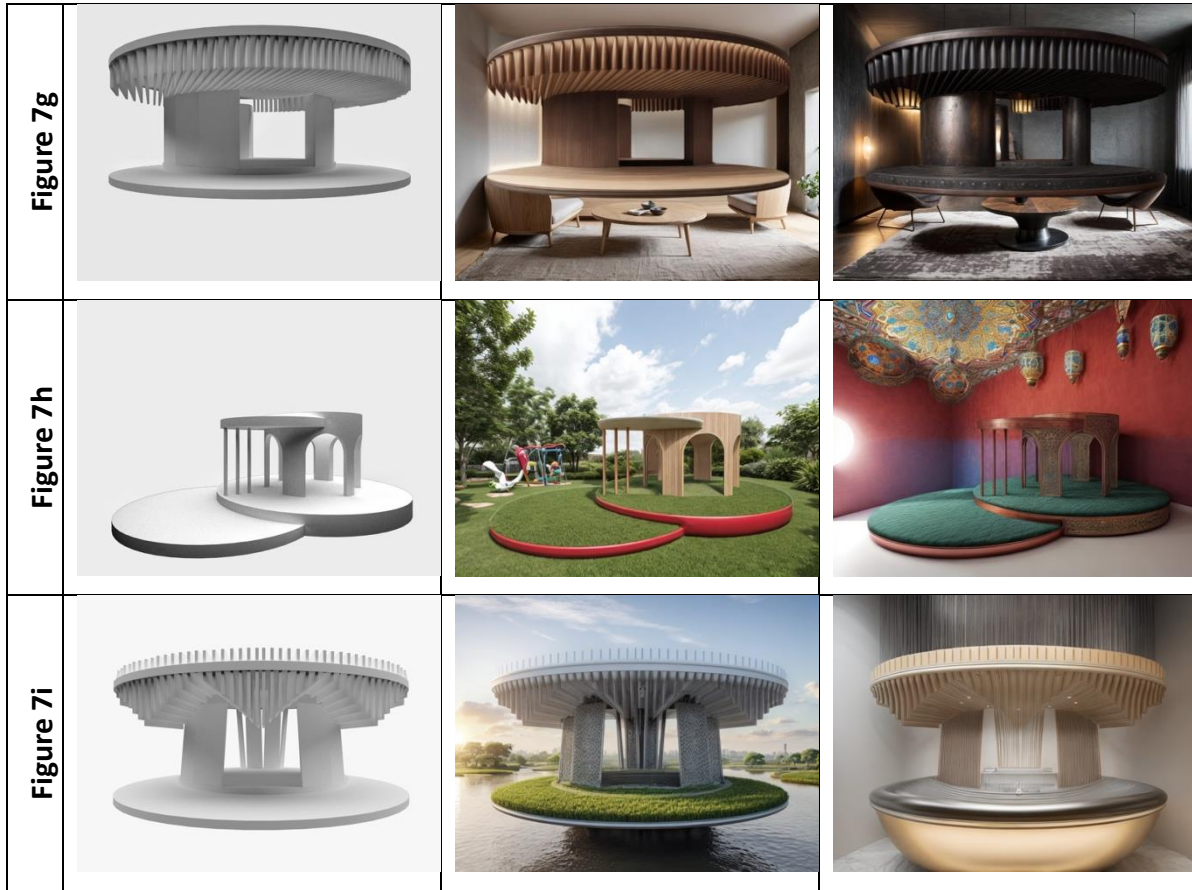


**Fig 7.** Figures of the approaches in which the forms were functionalized with the AI program PromeAI within the scope of the study


#### 4. CONCLUSIONS


Music and AI can be used together to create concepts and alternatives in spatial design approaches. In this context, suggestions on the contribution of music to the spatial design process are presented below:


- After examining the selected music piece or notes, the emotions and atmosphere expressed by the music can be reflected in the interior and exterior design using AI programs by considering elements such as tempo, rhythm, tone, harmony.
- The tones and rhythm of the music can determine the color scheme and lighting of the space. A lively and energetic piece of music can be associated with bright colors and dynamic lighting, while a softer and more emotional piece of music can be paired with colors that have calmer and softer tones. This can be made more emphatic through AI programs.
- The rhythm and flow of a piece of music can influence the layout of the space. For example, the rhythmic structure of the music can be a guide in determining the furniture layout or circulation routes within the space. Therefore, using AI programs can create a more remarkable space design.
- The tones of the instruments or notes in the music track can be a source of inspiration in the selection of materials to be used for the space. Thus, it can be stated that the emotions given by the music track can affect the overall feeling of the space when supported by AI programs.

It can be stated that as a result of the use of AI, which is used in many fields today, together with music in spatial design processes, many alternatives with faster and different features can be developed. AI, which is a current issue, can be considered as an approach that will enable the designer to reveal approaches at different scales and in different concepts. In conclusion, integrating AI and music offers the potential to develop innovative and practical approaches to spatial design.

## ORCID

Hüseyin Samet AŞIKKUTLU  <https://orcid.org/0000-0002-3518-7202>

Latif Gürkan KAYA  <https://orcid.org/0000-0001-8033-1480>

Betül Halime UZUNAY  <https://orcid.org/0000-0002-1007-6389>

## REFERENCES

- [1]. Welch, G.F., Biasutti, M., MacRitchie, J., McPherson, G.E., & Himonides, E. (2020). Editorial: the impact of music on human development and well-being. *Frontiers in Psychology*, 11, 1246. DOI: 10.3389/fpsyg.2020.01246
- [2]. Sloboda, J.A. (2010). Music in everyday life: the role of emotions. Juslin, P.N., Sloboda, J.A. (eds.), In *Handbook of Music and Emotion: Theory, Research, Applications*, (pp. 493–514). Oxford University Press.
- [3]. İmik, Ü., & Haşhaş, S. (2020). What is music and where is it in our lives. *İnönü University Journal of Culture and Art*, 6(2), 196-202.
- [4]. Ölgen, B., & Öztürk, Ö.B. (2019). Tasarım ve müzik ilişkisinin mekândaki izdüşümü. *Sanat ve Tasarım Dergisi*, 24, 301-319.
- [5]. Clerc González, G. (2003). *La arquitectura es música congelada*. (Doctoral dissertation), Escuela Técnica Superior De Arquitectura De Madrid, (10.08.2024). Retrieved from <https://oa.upm.es/268/>.
- [6]. Yılmaz, Y. (2008). *An approach to generate form in the intersection of music and architecture*. (Master's dissertation), İstanbul Technical University.
- [7]. Egido Jiménez, H. (2017). *Del tiempo al espacio. Diccionario Gráfico Comparado Entre Música y Arquitectura*. Trabajo Fin de Grado. ETSAM: Escuela Técnica Superior de Arquitectura de Madrid, (10.05.2024). Retrieved from <https://oa.upm.es/50857/>.
- [8]. Stretto House, (05.09.2024). Retrieved from <https://www.architectmagazine.com/project-gallery/stretto-house-506>.
- [9]. Borana, J. (2016). Applications of artificial intelligence & associated technologies. *Proceeding of International Conference on Emerging Technologies in Engineering, Biomedical, Management and Science [ETEBMS-2016]*, 5-6 March 2016. Jodhpur, India, pp. 64-67.
- [10]. Ghosh, M., & Thirugnanam, A. (2021). Introduction to artificial intelligence. Srinivasa, K.G., Siddesh, G. M., Mani Sekhar, S.R. (eds.), In *Artificial Intelligence for Information Management: A Healthcare Perspective*. *Studies in Big Data*, vol 88. Springer, Singapore. pp. 23-44. DOI: 10.1007/978-981-16-0415-7\_2
- [11]. Lukovich, T. (2023). Artificial intelligence and architecture towards a new paradigm. *YBL Journal of Built Environment*, 8(1), 30-45.
- [12]. Gelişen Tasarım: Yapay Zekâ ile Mekân Yerleşimi Üretimi, (06.09.2024). Retrieved from <https://xxi.com.tr/i/gelisen-tasarim-yapay-zekâ-ile-mekân-yerlesimi-uretimi>.
- [13]. Tazefidan, C., Eşme, E., & Başar, M.E. (2022). A Literature Study on the Use of Artificial Intelligence Applications in the Field of Architecture. *International Congress on Art and Design Research. Art & Design-2022 Book of Proceedings*, 20-21 June 2022. Kayseri, Türkiye, pp. 986-1002.
- [14]. Yıldırım, B., & Demirarslan, D. (2020). Evaluation of the benefits of artificial intelligence applications to the design process in interior architecture. *Humanities Sciences (NWSAHS)*, 15(2), 62-80. DOI: 10.12739/NWSA.2020.15.2.4C0236.
- [15]. Bayrak, E. (2022). *Evaluation of artificial intelligence and space design interaction in today's design education*, (Master's dissertation), Hacettepe University.
- [16]. *The Shape of Song*, (05.09.2024). Retrieved from <https://www.bewitched.com/song.html>.
- [17]. Wattenberg, M. (2002). Arc diagrams: visualizing structure in strings. *IEEE Symposium on Information Visualization, 2002, INFOVIS 2002*, 28-29 October 2002. Boston, MA, USA, pp. 110-116.